UNIVERSIDADE DE LISBOA
FACULDADE DE CIÊNCIAS
DEPARTAMENTO DE BIOLOGIA VEGETAL

Ovarian cancer organoids for modeling drug response and discovering novel BRCA biomarkers

Beatriz Pinto Galvão

Mestrado em Biologia Molecular e Genética

Dissertação orientada por:
Doutora Noélia Custódio
Doutora Andreia Figueiredo

2020

Acknowledgements

Back when I was still on the second year of my Bachelor's degree I started thinking about what I wanted to do after I graduated. I knew I wanted to do a Master's degree that would get me closer to the Genetics or Molecular Biology areas and FCUL had just the right one. So then I went further into planning my future and decided to look for places where one could develop their Master's Project at and that's when I found iMM. I remember going through the list of projects available for that school year and thinking "This is it! This is where I want to do my project!". Fast-forward to 2 years later and I found myself getting accepted at Maria Carmo-Fonseca Lab! So I want to thank Professor Maria do Carmo Fonseca for giving me the chance to reach my goal of experiencing the life of a researcher at iMM. I would also like to thank everyone at Carmo-Fonseca Lab who, from day one, made me feel welcome and part of the team, and were always willing to help whenever necessary.

Of course this project couldn't have happened without the person behind it, Catarina Vale. Not only did she provide all our tissue samples, she also helped with the processing and performed the histological analysis. She always tried to come up with solutions to whatever problems we had and I'm very glad she never stopped replying to my constant texts with random questions about tumor histology! I definitely learned a thing or two about that from her and it was an absolute pleasure getting to work with Catarina. I also want to give a big shoutout to the people at Hospital CUF Descobertas involved in this project because none of it would've been possible without them.

This journey wasn't an easy one, there were many ups and downs, but my close friends and family were with me through it all, they believed in me and always cheered me on, so to them I leave here a very big and heartfelt "thank you".

Even though we had few interactions, my internal advisor, Dr. Andreia Figueiredo, was always available to help and I deeply appreciate her support and guidance.

And last but not least, my biggest and most special "thank you" belongs to my advisor, Dr. Noélia Custódio. Noélia and I embarked on this organoid adventure together, both being a little lost at first, yet with time and lots of reading and googling we (kind of) got the hang of it. When I first arrived at the lab, I didn't know much about lab work and techniques, just the basics you learn in practical classes. But Noélia taught me everything she knows, shared her little tricks and tips with me, and never once made me feel bad about failing or making a mistake. She always tried to answer all my questions as best as she could and explain things as many times as necessary until I understood. Noélia did more for me than I could've ever asked for and through the good and bad times I knew I could count on her. There's no one else I'd rather have had alongside me during this journey and I'm incredibly grateful I got to know, work with and learn from such an incredible person. And no matter where the future takes me, I'll forever remember my time at iMM and my amazing advisor Noélia!

Abstract

Ovarian cancer (OC) is a heterogeneous disease and represents the second leading cause of gynecologic cancer-associated death. Late presentation of the disease is frequent and is associated with a reduced survival rate partially justified by a limited offer of therapeutic options and a lack of predictive biomarkers. Treatment usually involves cytoreductive surgery, followed by adjuvant platinum-based chemotherapy, however most patients relapse, in many cases with platinum-resistant/refractory tumors. For high-grade serous ovarian carcinoma (HGSOC), the most common type of OC that frequently features defects in the homologous recombination repair (HRR) pathway, an alternative strategy relies on the use of poly[ADP-ribose] polymerase inhibitors (PARPi). These drugs induce synthetic lethality in tumors with homologous recombination deficiency (HRD), as is the case of HGSOC arising in the context of *BRCA1/2* mutations, since BRCA proteins play a crucial role in the repair of DNA damage via HRR. Nevertheless, it is not yet possible to predict if tumors will respond to the available treatment regimens. Additionally, pathobiology of OC is poorly understood, mainly due to limitations in the available study platforms. Cancer cell lines and patient-derived xenografts are the most commonly used model systems to study OC, yet they hold several drawbacks that make them ineffective research tools. Such obstacles can be overcome by the use of the organoid technology. Cancer organoids, particularly patient-derived tumor organoids (PDTOs) are three-dimensional cell cultures derived from primary tumor cells, capable of self-renewal and self-organization. PDTOs maintain the morphophysiological and functional characteristics of their source tumors and have been shown to recapitulate tumor response to therapy.

The goal of this project was to generate patient-derived ovarian cancer organoids to examine how their drug sensitivity profile compares to patients' clinical response and determine how it correlates to expression of *BRCA* mRNA in HGSOC. Due to sample availability we only succeeded in developing organoids of low-grade serous ovarian carcinoma (LGSOC), which lacks *BRCA* defects and HRD, as well as normal fallopian tube organoids as controls. Nonetheless, we showed that the established organoids recapitulate architectural and cytologic features of parent tissue, in addition to PAX8 and p53 protein expression pattern. The drug sensitivity profiles of the tumor organoids also reflected what is expected for LGSOC, with the platinum-based drug cisplatin and the PARPi olaparib displaying no effect on organoid viability. Taken together, the results here obtained further support the hypothesis that PDTOs faithfully recapitulate many characteristics of their source tumors and might be reliable platforms to evaluate tumor response to therapy. As HGSOC samples become available in the future, we expect to develop organoids from this OC type and show proof-of-principle that drug response and DNA repair activity correlate with the expression of *BRCA1/2* transcripts in the original tumors, thus opening the possibility that *BRCA* mRNA could be used as a novel predictive biomarker for high-grade serous ovarian carcinoma.

Keywords: Ovarian cancer (OC), Serous ovarian carcinoma, Patient-derived tumor organoids, Preclinical model, Drug response

Resumo

O cancro do ovário (OC, *ovarian cancer*) representa a segunda causa de mortalidade por cancros ginecológicos. Este tipo de cancro inclui um conjunto de patologias heterogéneas, cada qual com as suas características histológicas, comportamentos biológicos e perfis moleculares e genéticos. Os tumores epiteliais do ovário (EOC, *epithelial ovarian cancer*) são as neoplasias mais comuns e dividem-se em diversos tipos histológicos, dos quais os carcinomas serosos representam a maioria. Estes subdividem-se em carcinoma seroso de alto grau (HGSOC, *high-grade serous ovarian carcinoma*) e carcinoma seroso de baixo grau (LGSOC, *low-grade serous ovarian carcinoma*) que, embora pertençam ao mesmo subtipo, são neoplasias consideravelmente distintas, apresentando diferenças a nível histológico, bem como diferentes alterações genéticas e resposta à terapia.

O HGSOC é o carcinoma seroso mais comum, representando cerca de 90% dos casos. É geralmente diagnosticado num estádio avançado e, dada a escassez de opções terapêuticas, constitui a forma de OC mais letal. Pensa-se que estes tumores tenham origem em lesões precursoras do epitélio das fímbrias (zona distal das trompas de falópio) designadas de carcinomas serosos intraepiteliais tubários (STICs, *serous tubal intraepithelial carcinomas*). Um dos principais atributos do HGSOC são mutações no gene supressor de tumores *TP53* (97%), e perto de 20% dos casos estão associados a mutações na linha germinativa dos genes *BRCA1/2*. As proteínas BRCA são fundamentais para a reparação *error-free* de lesões no DNA por recombinação homóloga (HR, *homologous recombination*), pelo que em células deficientes em BRCA estes danos são reparados por mecanismos alternativos que introduzem erros no DNA e induzem instabilidade genómica, uma característica típica de HGSOC. Defeitos a nível da reparação de lesões por HR estão presentes em cerca de metade dos carcinomas de alto grau e são responsáveis pela eficácia da quimioterapia. O tratamento atual para EOC, incluindo HGSOC, consiste na cirurgia primária seguida de quimioterapia adjuvante à base de um composto de platina e paclitaxel. O dupleto padrão corresponde a carboplatina/paclitaxel, uma vez que a cisplatina inicialmente utilizada apresenta uma toxicidade acrescida. Estes agentes terapêuticos à base de platina atuam pela formação de ligações cruzadas entre bases do DNA que, quando ocorrem entre as cadeias antiparalelas (ICLs, *interstrand crosslinks*), impedem a sua separação, inibindo os processos de transcrição e replicação. Deste modo, garfos replicativos que encontrem uma ICL acabam por colapsar e originar *double-strand breaks* (DSBs). Nos casos em que as vias de reparação de lesões no DNA estão comprometidas, em especial a via de HR, estes danos não são reparados e a sua acumulação resulta na morte das células neoplásicas. No entanto, frequentemente as pacientes recidivam com tumores resistentes a platina pelo que se torna necessário recorrer a estratégias de tratamento alternativas. Na Europa é recomendado o uso de inibidores da PARP (PARPi) em doentes com mutações *BRCA* para tratamento das recidivas e como terapia de manutenção. Os PARPi induzem letalidade sintética em células com defeitos na HR, como acontece frequentemente no HGSOC. Estes fármacos inibem a reparação de *single-strand breaks* (SSBs), que permanecem por reparar e culminam no colapso dos garfos replicativos em DSBs; nas células em que a via de reparação por HR está comprometida, estas lesões não são reparadas e eventualmente as células morrem. A marcação imunohistoquímica nestes tumores é habitualmente positiva para WT1 (um marcador do tipo seroso) e PAX8 (um marcador de tecidos de origem Mülleriana que incluem a trompa de falópio), e o p53 apresenta uma marcação *"mutation-type"*, devido a mutações frequentes no gene que codifica esta proteína.

Por outro lado, o LGSOC representa apenas 10% dos casos de tumores serosos, e menos de 5% de todos os casos de EOC. É também muitas vezes diagnosticado tardiamente mas possui melhor prognóstico que o HGSOC. À semelhança dos carcinomas de alto grau, existe evidência que possam ter origem tubária, resultando da invaginação do epitélio das fímbrias no córtex ovárico. Esta invaginação leva à formação de inclusões no epitélio do ovário que progridem para tumores serosos *borderline* e, eventualmente, LGSOC. Estes tumores raramente apresentam mutações no *TP53* e nos genes *BRCA1/2*,

pelo que não é comum demonstrarem defeitos na via de reparação do DNA por HR, nem instabilidade cromossómica. As alterações genéticas mais frequentes consistem em mutações mutuamente exclusivas nos genes *KRAS*, *BRAF* e *ERBB2* que resultam numa ativação da via MAPK. Embora o LGSOC demonstre uma resposta relativamente reduzida à quimioterapia padrão, não existem outras estratégias de tratamento disponíveis para este tipo de cancro, e os PARPi não se aplicam devido à presença de HR funcional. É comum marcarem positivamente para WT1 e PAX8, e o p53 apresenta um padrão *wild-type*.

Um dos grandes obstáculos ao desenvolvimento de terapias anticancerígenas mais eficientes reside na inexistência de modelos tumorais que simulem o comportamento biológico *in vivo* dos mesmos. Linhas celulares cancerígenas e xenoenxertos provenientes de pacientes (PDXs, *patient-derived xenografts*) constituem os modelos mais utilizados no estudo do cancro, no entanto possuem várias características que os tornam ferramentas de investigação ineficazes. Recentemente, o uso de organoides surgiu como uma promissora alternativa aos modelos existentes. Os organoides, e em particular organoides tumorais provenientes de pacientes (PDTOs, *patient-derived tumor organoids*), são culturas celulares tridimensionais com origem em células tumorais primárias que, quando colocadas numa matriz extracelular com fatores de crescimento adequados, se renovam e organizam em estruturas semelhantes aos tumores originais. Os PDTOs já foram estabelecidos para diversos tipos de cancro, incluindo cancro do ovário, e são caracterizados por manterem vários aspetos chave dos seus tumores de origem, nomeadamente morfologia, perfis genéticos e heterogeneidade intra- e intertumoral. Além disso, em alguns casos, a resposta a fármacos nestes organoides refletiu a dos pacientes, pelo que demonstram elevado potencial como um modelo a ser usado para avaliar a resposta de tumores individuais ao tratamento, podendo permitir, futuramente, a obtenção de regimes terapêuticos adaptados a cada paciente.

O objetivo deste projeto consistiu em desenvolver organoides de tumores de ovário, em particular do tipo seroso de alto grau, para avaliar de que modo os seus perfis de resposta a fármacos se correlacionam com a resposta dos pacientes, bem como com a expressão de *BRCA* nos tumores originais, e era esperado que estes transcritos pudessem representar um novo marcador preditivo de resposta para HGSOC. No entanto, devido à falta de amostras, apenas foi possível gerar organoides de um LGSOC e de trompa de falópio como controlo. Ainda assim, mostrou-se que, à semelhança de descrições anteriores, estes organoides tumorais revelaram semelhanças histológicas com o seu tumor de origem, nomeadamente padrões de expressão de WT1, PAX8 e p53. Também se demonstrou que a arquitetura estrutural dos organoides de LGSOC é distinta da dos de trompa de falópio, e ambas se assemelham à organização espacial do tecido original. Relativamente à sensibilidade a fármacos, os perfis de resposta dos organoides de LGSOC à cisplatina e ao PARPi olaparib refletiram o que é expectável para este tipo de tumor, que regra geral não responde à quimioterapia com compostos de platina e em que a inibição da PARP não surte qualquer efeito anti tumoral. Já os organoides de trompa de falópio revelaram a acrescida toxicidade da cisplatina relativamente à carboplatina, em que concentrações elevadas da primeira levaram a uma redução drástica na viabilidade dos organoides.

Em suma, os resultados obtidos suportam a hipótese de que os PDTOs replicam muitas das características dos seus tumores de origem e que poderão constituir um modelo pré-clínico para avaliar a resposta dos mesmos à terapia. Espera-se que no futuro, com a disponibilidade de amostras de HGSOC para desenvolvimento de organoides tumorais, nos seja possível correlacionar a resposta a fármacos e a capacidade de reparação do DNA nos mesmos com as isoformas e níveis de expressão de *BRCA1/2* nos tumores originais. Os transcritos de *BRCA* poderão, então, representar potenciais biomarcadores de previsão de resposta a fármacos em carcinomas serosos de alto grau.

Palavras-chave: Cancro do ovário, Carcinoma seroso do ovário, Organoides tumorais provenientes de pacientes, Modelo pré-clínico, Resposta a fármacos

Contents

List of Figures

List of Abbreviations

ADP	Adenosine diphosphate
ACK	Ammonium-Chloride-Potassium
ATM	Ataxia-telangiectasia mutated
ATR	ATM- and Rad3-Related
BER	Base excision repair
BME	Basement Membrane Extract
BMP	Bone morphogenic protein
BRAF	V-raf murine sarcoma viral oncogene homolog B
BRCA	BReast CAncer gene
BSA	Bovine Serum Albumin
CA-125	Cancer antigen 125
CC1	Cell Conditioning 1
CIC(s)	Cortical inclusion cyst(s)
CNA(s)	Copy number alteration(s)
DAPI	4′,6-diamidino-2-phenylindole
DDR	DNA damage response
DMEM	Dulbecco's Modified Eagle Medium
DNA	Deoxyribonucleic acid
DNase	Deoxyribonuclease
DNA-PK	DNA-dependent protein kinase
DPBS	Dulbecco’s Phosphate-Buffered Saline
DSB(s)	Double-strand break(s)
ECM	Extracellular matrix
EGF	Epidermal growth factor
EHS	Engelbreth-Holm-Swarm
EOC	Epithelial ovarian cancer
EpCAM	Epithelial cell adhesion molecule
ER	Estrogen receptor
ERBB2	V-erb-b2 avian erythroblastic leukemia viral oncogene homolog 2
FA	Fanconi anemia
FBS	Fetal Bovine Serum
FGF	Fibroblast growth factor
FT	Fallopian tube
G-418	Geneticin
H_20	Water
H&E	Hematoxylin & Eosin
HE4	Human epididymis protein 4
HEPES	4-(2-hydroxyethyl)-1-piperazineethanesulfonic acid
HGSOC	High-grade serous ovarian carcinoma
HR	Homologous recombination
HRD	Homologous recombination deficiency
HRR	Homologous recombination repair
ICL(s)	Interstrand cross-link(s)
IF	Immunofluorescence
IHC	Immunohistochemistry
KRAS	Kirsten rat sarcoma viral oncogene homolog

LGSOC	Low-grade serous ovarian carcinoma
MAPK	Mitogen-activated protein kinase
mg	Milligram
mL	Milliliter
mM	Millimolar
MMR	Mismatched repair
mRNA	Messenger ribonucleic acid
NER	Nucleotide excision repair
ng	Nanogram
NHEJ	Non-homologous end joining
OC	Ovarian cancer
OEI(s)	Ovarian epithelial inclusion(s)
OSE	Ovarian surface epithelium
PAR	Poly ADP-ribose
PARP	Poly[ADP-ribose] polymerase
PARPi	Poly[ADP-ribose] polymerase inhibitors
PAX8	Paired box gene 8
PBS	Phosphate-Buffered Saline
PDTO(s)	Patient-derived tumor organoid(s)
PDX(s)	Patient-derived xenograft(s)
Pen-Strep	Penicillin-Streptomycin
PFA	Paraformaldehyde
ROCK	Rho kinase
R-Spondin1	Roof plate-specific Spondin-1
SBT(s)	Serous borderline tumor(s)
SSB(s)	Single-strand break(s)
STIC(s)	Serous tubal intraepithelial carcinoma(s)
TP53	Tumor protein 53
UK	United Kingdom
USA	United States of America
UV	Ultraviolet
WHO	World Health Organization
WT1	Willms' tumor 1
µL	Microliter
µm	Micrometer
µM	Micromolar

1. Introduction

In 2018, ovarian cancer (OC) was the eight most common cancer worldwide in women, the eight leading cause of cancer-associated death, and the second most fatal gynecologic malignancy (after cancer of the cervix uteri) [1]. Although commonly thought of as a single disease, ovarian cancer is actually a group of heterogeneous diseases, each with their own histological features, biological behavior, and genetic and molecular profile [2,3]. There are different types of cells present in the ovary and they can all originate neoplasms. Ergo, most primary ovarian tumors can be grouped into one of three major types: epithelial, germ cell, and sex-cord-stromal [4,5]. Epithelial ovarian cancer is the most common type and, since being the focus of this project, will be the only one covered here.

1.1. Epithelial ovarian cancer

Epithelial ovarian cancer (EOC) accounts for about 95% of all ovarian tumors [3,5]. According to the WHO, epithelial tumors can be categorized into six main histological subtypes, namely serous, mucinous, endometrioid, clear cell, seromucinous and Brenner [6]. Serous carcinomas comprise the majority of malignant EOC and are further subdivided into high-grade serous (HGSOC) and low-grade serous (LGSOC) [5–7]. HGSOC is the most common histological subtype, accounting for around 75% of all EOC, while LGSOC represents less than 5% [5,8]. Although being included in the same category of serous tumors, HGSOCs and LGSOCs are strikingly distinct diseases, with differences in histology, molecular genetic alterations, etiology, response to treatment and prognosis [2,5,9].

1.1.1. High-grade serous ovarian carcinoma

HGSOC is the most frequent of the serous subtype, making up 90% of all cases [5,10,11]. Over 75% of patients are diagnosed at an advanced stage, mostly due to an absence of symptoms which, together with the lack of effective screening methods and available treatment options, result in HGSOC being the most lethal form of OC, with a 5-year survival rate of around 46% [3,4,8,11]. A distinctive hallmark of HGSOC are mutations in the tumor suppressor gene *TP53*, present in close to 97% of these tumors [3]. This gene encodes for p53, a transcription factor that plays an important role in the cellular response to DNA damage, the regulation of the cell-cycle and apoptosis [12]. The majority of HGSOCs are sporadic but 15% to 20% of the cases are associated with germline mutations in genes involved in repairing DNA lesions through homologous recombination (HR), namely *BRCA1* and *BRCA2* [3,13]. Besides inherited mutations, inactivation of the BRCA pathway can also occur due to somatic mutations in either of the *BRCA* genes or, in the case of *BRCA1*, through an epigenetic mechanism of promoter hypermethylation [3,10]. BRCA proteins are essential for the error-free repair of double-strand breaks (DSBs) on DNA through HR. However, in BRCA-deficient cells these lesions are repaired by alternative mechanisms that are potentially error-prone and promote chromosomal instability [14]. Therefore, genomic instability, and the consequent accumulation of copy number alterations (CNAs), are typical characteristics of high-grade carcinomas [3,11]. A defective homologous recombination repair (HRR) pathway results from inactivation of the *BRCA* genes, and related ones, and is found in approximately 50% of HGSOCs [2,11]. This HR deficiency (HRD) is a key factor for the effectiveness of chemotherapy, as well as for the development of alternative treatment strategies, and will be reviewed in a later chapter.

Microscopically, HGSOCs have a certain degree of intra- and inter-tumoral heterogeneity, showing distinct morphological patterns that include papillary, micropapillary, glandular and cribriform. They typically present as solid masses of cells with slit-like fenestrations, and these areas frequently appear with regions of necrosis. The tumoral cells show large and pleomorphic nuclei, prominent nucleoli, and usually have a high mitotic index with many visible mitotic figures that are

commonly abnormal [2,11,13,15]. Immunohistochemistry staining is normally positive for WT1 (a marker of the serous subtype), p16 and PAX8 (a marker of tissues of Müllerian origin which include the fallopian tube) [13,15,16]. Since most HGSOCs have *TP53* mutations, p53 staining is usually "mutation-type" (abnormal staining) and the pattern of expression depends on the type of mutation: missense mutations lead to a strong and diffuse nuclear staining in most cells, since the mutant p53 proteins cannot be degraded by the proteasome and accumulate in the nucleus; on the other hand, nonsense mutations, indel, and splicing mutations lead to an almost totally negative staining (the "null-pattern") because the protein is absent or its truncated forms are not recognized by the antibodies targeting p53 [2,13,15]. The high proliferation rate of these tumors is reflected in an elevated nuclear expression of Ki-67 [2,8]. Over 70% of high-grade carcinomas also stain positive for the estrogen receptor (ER) [2,13].

Unlike most types of EOC, the precise origin of HGSOC remains to be determined [13,17]. Initially, it was thought that HGSOC originated in the ovarian surface epithelium (OSE). The constant cycles of ovulation could potentiate a pro-inflammatory and pro-oxidative microenvironment, leading to DNA damage, which, if not repaired adequately, could promote carcinogenesis [13,17]. This incessant cycling of repair of the OSE results in certain regions invaginating and becoming trapped under the ovarian surface in structures called cortical inclusion cysts (CICs), which are likely to have oncogenic potential [10,13,18]. However, recent evidence supports the hypothesis that this type of cancer might actually arise from secretory epithelial cells of the fimbriae, the distal portions of the fallopian tubes [9,15,19]. This hypothesis was put forth after being found that a large majority of women with a hereditary predisposition for developing HGSOC due to *BRCA* mutations, who underwent risk-reducing salpingo-oophorectomy, had precursor lesions in the fimbriae known as serous tubal intraepithelial carcinomas (STICs) [3,15,18]. STICs originate from the normal fallopian tube epithelium which, similarly to the OSE, is repeatedly exposed to inflammatory cytokines during ovulation; such microenvironment causes DNA damage and ultimately might lead to mutations in *TP53* [17]. These secretory epithelial cells with mutated p53 proteins are termed "p53 signatures" and are characterized by more than 12 consecutive cells with a morphologically normal appearance but a high proliferative capacity and a "mutation-type" p53 staining [15,17,19]. As p53 signatures acquire more mutations and proliferate, they originate STICs, which progress and are exfoliated from the fimbriae. Eventually these invading cells reach the ovarian surface and transform into HGSOC [17]. Basically all high-grade carcinomas have somatic mutations in *TP53* and many of these are shared by p53 signatures and STICs, indicating a common origin for all three entities [18,19].

As mentioned before, there are no effective screening strategies that allow for the detection of HGSOC at early stages [13]. The cancer antigen 125 (CA-125), a membrane-bound glycoprotein expressed by neoplastic cells of many EOCs, has been widely used as a tumor marker for ovarian cancer [5,20,21]. Serum levels of CA-125 are commonly elevated in advanced cases, however, this marker has been found to lack specificity and sensitivity, making it unsuitable as a screening method on its own [5,13,22]. Nevertheless, it has been reported that blood levels of CA-125 in combination with other tools, such as transvaginal ultrasonography, may be helpful in detecting high-grade carcinoma, as well as other types of EOC [5,13]. Further biomarker combinations have been tested along with CA-125, in particular the human epididymis protein 4 (HE4), a secretory protein originally found in the epithelial cells of the human epididymis, which is overexpressed in EOC [5,8,23,24]. Nonetheless, additional studies are needed to understand the advantage of using said combination for the early diagnosis of ovarian cancer [8,23].

Standard treatment for patients with HGSOC, as for all EOC, consists on primary debulking surgery, followed by adjuvant chemotherapy [4,7]. The goal of cytoreductive surgery is to resect all tumor masses, including those which have spread to the peritoneal cavity of the patient, so that no residual tumor remains [13]. In some cases, it may be necessary to diminish tumor burden before

surgery with neoadjuvant chemotherapy [5,7]. Irrespective of its type, standard-of-care therapeutic for EOC is commonly known as a platinum-based therapy, and consists in the combination of a platinum-based drug with a taxane [3,5,7,13]. The first platinum agent to be used was cisplatin, yet it was later replaced by carboplatin since the latter is far less toxic, while equally effective [4,7,13]. Carboplatin is usually combined with the taxane paclitaxel, and this represents the standard first-line therapeutic for advanced-stage EOC patients [3,5,7,8]. The cisplatin/paclitaxel duplet might still be administered but only to patients with a hypersensitivity to carboplatin [4]. Although most patients respond favorably to first-line chemotherapy, over 75% will eventually relapse [4,13]. In the case of platinum-sensitive cancers, follow-up treatment usually follows the same platinum/taxane regimen as first-line therapy [8,13]. However, if tumors are platinum-resistant or refractory, alternative strategies need to be implemented [4,13]. Targeted drugs are thus becoming increasingly more relevant as maintenance therapy of recurrent ovarian cancer, namely the anti-angiogenic agent bevacizumab and PARP (poly[ADP-ribose] polymerase) inhibitors (PARPi) [3,4]. Bevacizumab was the first anti-angiogenic agent to show positive results in the treatment of both platinum-sensitive and resistant relapses, together with chemotherapy, and as a single-agent for maintenance therapy [4]. PARPi are a class of drugs whose mode of action exploits defects in HR. Ergo, they have been successfully employed in treatment of recurrent HGSOC and as maintenance therapy, since HRD is seen in half of these cancers, frequently due to mutations in *BRCA1/2* [3,4,8]. Olaparib was the first PARPi to be approved, and the European medical guidelines recommend its use in women with platinum-sensitive recurrent disease and *BRCA1* or *BRCA2* mutations. Other PARPi, like niraparib and rucaparib, have been shown to be effective in prolonging progression-free survival in both *BRCA*-mutant and wild-type patients, with a greater benefit to the former [7,13]; therefore they have been approved in the United States of America to treat HGSOC patients irrespective of *BRCA*-mutation status or platinum-sensitivity [13]. The relation between PARPi and HRD will be enlightened later on.

1.1.2. Low-grade serous ovarian carcinoma

LGSOC is rare, representing only about 10% of serous ovarian tumors and less than 5% of all EOC cases [2,25,26]. Similar to HGSOC, around 70% of these tumors are diagnosed at an advanced stage, although low-grade carcinomas have a better prognosis, with a 5-year survival rate of approximately 54%. LGSOC usually presents in younger women when compared with HGSOC (47 years vs 63 years) [27]. The mutational profile also differs from that of high-grade carcinomas as *TP53* mutations are virtually inexistent and patients rarely carry pathogenic mutations in *BRCA1/2* [3,27]. Instead, LGSOCs commonly feature an activated MAPK pathway, detected in up to 80% of these tumors, which results from mutually exclusive mutations in *KRAS*, *BRAF* and *ERBB2*. Low-grade tumors tend to be genetically stable and have less CNAs than their high-grade counterparts [3,11,26,28].

Histologically, LGSOCs are less heterogeneous, typically characterized by micropappilae and small round nests of cells that randomly infiltrate the stroma, being often surrounded by clear clefts. Tumor multinucleated giant cells and necrosis are not usually present in these carcinomas [25,28]. Neoplastic cells have small, round to oval, uniform nuclei, usually their distinguishing feature from HGSOCs, and their proliferation rate is lower, with infrequent mitotic figures [2,28]. Immunohistochemical staining is commonly positive for WT1, PAX8 and ER but negative for p16 [16,28,29]. p53 staining follows a wild-type pattern which consists of a heterogeneous nuclear staining, with either a few positive cells or nearly all cells positive but with variable intensity [15]. Ki-67 labelling is reduced, reflecting the fairly slow growth of LGSOCs [2,26,28].

The most widely accepted model for the origin of LGSOCs is that these are formed in a stepwise fashion from ovarian epithelial inclusions (OEIs) to benign serous cystadenomas, and then to serous borderline tumors (SBTs), which may eventually progress to low-grade serous carcinomas [26,30,31]. In some cases it is believed that this progression is actually from reccurence of previously

detected or undetected SBTs [11,26]. Although their name suggests an ovarian origin, recent findings have provided strong evidence that the majority of OEIs are, in fact, fallopian tube-derived [30,31]. Therefore, LGSOC, similarly to HGSOC, most probably derives from the fallopian tube rather than the ovarian surface epithelium. The proposed sequence of low-grade carcinoma development begins with the fallopian tubal epithelium, in particular the fimbriated end, adhering to the ovarian surface. This is likely facilitated by the close spatial proximity between the fimbriae and the ovary, as well as ovulation and nonovulation-induced disruption of the ovarian surface. The implanted fallopian tubal epithelium can then invaginate into the ovarian cortex and originate tubal-derived OEIs. These aquire mutations in genes like *KRAS* or *BRAF*, and progressively transform into SBTs and, ultimately LGSOCs [30,31].

Screening of LGSOC is no different from that of most EOC and, like for HGSOC, also includes the evaluation of serum CA-125 levels, which are typically lower in patients with low-grade tumors [32].

As mentioned previously, typical treatment for EOC, and hence LGSOC, relies on primary debulking surgery followed by a platinum/taxane-based chemotherapy regimen, usually carboplatin/paclitaxel [25,26,32]. However, low-grade carcinoma is relatively insensitive to chemotherapy, with reports of its response to carboplatin/paclitaxel in previously untreated cases being less than 25% [26,27]. Although the chances of achieving a status of no residual disease after primary cytoreductive surgery are higher than in HGSOCs, low-grade cancers might eventually recur [26,27]. Despite its inherent chemoresistance, reccurent disease is usually treated with standard-of-care chemotherapy, since no other effective therapeutic strategies are currently available for clinical use [26,27]. Nevertheless, there are several alternative treatments being evaluated. As for HGSOC, the use of bevacizumab in combination with normal chemotherapy or as monotherapy has been reported to potentially improve outcome in LGSOC [25,27]. Seeing that most low-grade tumors express ER and PR, hormonal treatment has been considered as an alternative to chemotherapy for recurent cases or as maintenance therapy, but further studies need to be conducted in order to evaluate its efficacy over standard-of-care therapeutics [25–27]. A different treatment strategy takes advantage of the mutations in the MAPK pathway commonly present in LGSOC, with agents targeting and inhibiting this pathway having therapeutical potential [26–28,32].

1.2. DNA damage response in the context of ovarian cancer treatment

Cancer cells are known to have a higher extent of DNA lesions than normal cells [33]. This fact, taken together with their inherent inability to repair such DNA damage, results in many tumors being genetically unstable [34,35]. Usually defective in cancer, one of the main contributors to maintaining genome integrity is the DNA damage response (DDR) [35]. DDR is triggered in the presence of DNA lesions, either endogenous or exogenous, and involves the activation of a network of cellular signaling events aimed at slowing down or halting DNA synthesis, blocking the cell cycle, and activating repair pathways [35].

Normally, DNA damage originates either single-strand breaks (SSBs) or double-strand breaks (DSBs), with the former being the most common endogenous lesions [33,34]. There are five main mechanisms for DNA repair, namely mismatch repair (MMR), nucleotide excision repair (NER), and base excision repair (BER) for SSBs and non-homologous end joining (NHEJ) and homologous recombination repair (HRR) for DSBs [34]. MMR is responsible for repairing incorrect base matches (mismatches) and nucleotide insertion/deletion errors generated during replication [33,34,36]. NER is a highly conserved and versatile pathway responsible for the removal of “bulky lesions”, like the ones caused by UV radiation, which distort the DNA double helix. This pathway also contributes to the repair of intrastrand and interstrand crosslinks (ICLs), including those caused by platinum agents used in chemotherapy [33–35], which will be reviewed later. BER is responsible for removing small base lesions caused by reactive oxygen species or alkylation, and for repairing the common SSBs [34,37]. Damaged

bases are removed, then the DNA section containing the lesion is excised and new undamaged DNA is synthetized, a process to which enzymes of the poly(ADP-ribose) polymerase (PARP) family, namely PARP1 and PARP2, are essential [37,38]. This pathway has become the focus of a new category of alternative cancer drugs, PARPi, whose mode of action will be explained in a later chapter. NHEJ is considered to be the simplest and rapidest mechanism to repair DSBs which, though being less common, are the most difficult DNA lesions to repair, as well as the most cytotoxic [33,39]. This pathway promotes DNA repair by directly linking the ends of a DSB together, regardless of sequence homology, making it error-prone because it can cause the deletion or mutation of DNA sequences surrounding the break [37,39,40]. NHEJ is active throughout the cell cycle but predominates during the G0 and G1 phases [33,36,39]. Contrary to NHEJ, HRR is highly complex and the most accurate mechanism for repairing DSBs or stalled and collapsed replication forks [33–35,39]. In this pathway DNA strand homology is needed for the repair of DNA damage, with the broken ends of a DSB being resected to allow for their invasion into the sister chromatid that acts as a template for error-free resynthesis of the damaged region [33,39]. Since the presence of a sister chromatid is required, HRR is only active during the S and G2 phases of the cell cycle [36].

Most of the therapeutic strategies being currently used in ovarian cancer, be them standard-of-care or alternative, take advantage of the tumors' inherent defects in the DDR. The following chapters describe the relation between OC therapy and DNA repair mechanisms.

1.2.1. Platinum-based drugs: cisplatin and carboplatin

As mentioned before, typical treatment for EOC consists of drug combinations containing platinum-based agents, mainly carboplatin and cisplatin. These are cross-linking agents that exert their cytotoxic effect by covalently binding to guanines in DNA and generating DNA adducts [35,41,42]. These DNA adducts can cross-link bases on the same strand, forming intrastrand crosslinks (the most common), or on opposite strands, forming interstrand crosslinks (ICLs, the most cytotoxic and the ones responsible for the antitumoral action) [35,42]. Because ICLs bind both DNA strands together, their separation is prevented which, in turn, leads to a block of transcription and replication [36,42]. Moreover, replication forks that meet an ICL become stalled and may eventually collapse, originating DSBs [36]. If DDR is impaired then these lesions cannot be resolved and tend to accumulate, resulting in cell death [36].

Intrastrand crosslinks are mainly repaired through NER. Resolution of ICLs, on the other hand, requires a combination of several repair mechanisms, specifically NER, HRR and the Fanconi Anemia (FA) pathway [35,42]. ICL repair via the FA pathway involves the intervention of several proteins that also play a role in HRR, like BRCA1/2 [43,44]. Ovarian tumors frequently show HRD, mostly HGSOCs, which makes them particularly sensitive to platinum-based drugs [33,37]. As previously stated, approximately 50% of HGSOCs have defects in HRR and up to 20% are due to inherited mutations in the *BRCA* genes [2,3,11,13]. In fact, it has been reported that ovarian cancer patients with *BRCA1/2* mutations have higher rates of platinum sensitivity when compared to *BRCA* wild-type patients [41]. It has also been shown that NER defects are present in around 8% of EOC and these alterations were associated with better patient outcome, their survival being comparable to that of *BRCA*-mutation carriers [34,35]. This suggests that impairment of NER in ovarian cancer might confer platinum sensitivity to a similar extent as that of HRD resulting from BRCA inactivation [34,35].

1.2.2. PARPi

It is now widely known that a defective HRR pathway, mostly due to inactivation of BRCA proteins, renders cancer cells sensitive to PARPi, which exert their action by inducing synthetic lethality in such cells [33]. Synthetic lethality occurs when defects in one gene or protein do not affect cell viability but in combination with other defects result in cell death [45]. In the case of PARP

inhibition this is achieved by inhibiting BER in cells already defective in HRR [34]. When a SSB is detected, PARP1 binds DNA at the site of the break and synthetizes PAR chains (PARylation) on several proteins that will act as a scaffold for effectors of BER. PARP1 eventually autoPARylates and is released from DNA, allowing the repair process to occur [45]. Drug-like small molecule inhibitors of PARP1, which also inhibit PARP2, prevent catalytic activity and promote an allosteric conformational change that traps PARP enzymes at SSBs [33,46]. Therefore, these lesions remain unrepaired and persist, causing replication forks to stall and possibly collapse into DSBs. In HRR-defective cells such stalled/collapsed replication forks and DSBs cannot be repaired, or are repaired by the error-prone NHEJ pathway, which leads to chromosomal instability, cell-cycle arrest and ultimately cell death [33,34,41,46].

The efficacy of PARPi is not limited to ovarian cancers with germline *BRCA* mutations [38]. In fact, sporadic cancers with somatic inactivation of *BRCA* have also shown sensitivity to these drugs [33]. Moreover, HRD arising in other genetic alterations has been reported to confer PARPi sensitivity, which further expands their use as a treatment strategy beyond *BRCA*-mutated EOC [33].

1.3. Patient-derived organoids as cancer models

Although extensive advances have been made in cancer treatment strategies over the last decades, this disease still remains one of the greatest challenges for human health [47,48]. Worldwide, cancer is responsible for 1 in every 6 deaths, with an estimated 9.6 million deaths in 2018 [49]. Such burden could be reduced with the development of more effective and targeted therapies, which should take into account the high degree of tumor heterogeneity seen between and within individual patients [50]. However, cancer models currently available fail to mimic the biological behavior of *in vivo* human tumors, making them unsuitable for an accurate screening of potential new anti-cancer drugs [47]. Thus, improved preclinical cancer models are needed to better understand how each individual tumor responds to treatment, allowing for personalized therapeutic strategies over the usual "one-size-fits-all" approach.

Cancer cell lines and patient-derived xenografts (PDXs) are commonly used as human cancer models for drug screening and evaluating drug responses [48]. Cancer cell lines are derived from primary patient tumors and have been of great value to cancer research [47,48]. They are easy to maintain and expand quickly, with little associated costs, having been widely used for high-throughput screening of potential drugs and cancer biomarkers [48,50]. Nevertheless, these cell lines can only be generated from a limited number of cancer subtypes and they acquire morphological and genetic modifications due to positive clonal selection after many passages in FBS-based cultures, making them lose the specific heterogeneity of the original tumors [50–52]. As a result, many pharmacological compounds that perform well in cancer cell lines end up showing toxicity and lack of efficacy in clinical trials [53]. PDXs are generated by transplanting fresh tumor fragments subcutaneously or orthotopically into immunodeficient mice [47,48]. Therefore, they retain most histological and genetic features of their tumors of origin, and are known to share a similar drug response to that observed in clinical settings, with a high correlation between therapeutic efficacy in PDXs and patients having been reported [51,52]. However, alike cancer cell lines, it is still difficult to efficiently develop PDXs from certain tumor types [51], and they might undergo mouse-specific tumor progression [47]. Moreover, PDXs are expensive, as well as resource and time-demanding, making this model incompatible with high-throughput drug screenings [50,54].

Recently, a new technology has emerged that holds great promise for translational cancer research: the organoid technology [50]. Organoids can be defined as three-dimensional structures that grow from stem cells, consisting of organ-specific cell types which self-organize through cell sorting and spatially restricted commitment [55]. These cells are cultured in a substitute of extracellular matrix and, with the appropriate growth factors in order to mimic stem cells niches, differentiate and form organized tissues with different types of epithelial cells and a spatial architecture that resembles that of

the original tissues, healthy or diseased [53–55]. Tumor organoids, more specifically patient-derived tumor organoids (PDTOs), can thus be developed from resected primary tumor samples, as well as from ascites, pleural effusions and metastatic lesions [51,56]. These PDTOs are capable of self-renewal and self-organization, and have been shown to retain key aspects of primary tumors, including histological and molecular profiles, genomic and transcriptomic alterations, as well as intra- and intertumoral heterogeneity [48,51,56,57]. Furthermore, several studies have evidenced that tumor organoids can be used for *in vitro* drug sensitivity assays, with their response being, in most cases, predictive for patients' responses to therapy. Therefore, PDTOs appear more advantageous over other tumor models, especially regarding their use in the context of personalized medicine as a platform for predicting therapy response [51,58].

1.3.1. Patient-derived ovarian cancer organoids

PDTOs have been established for several types of human cancer [59], and ovarian cancer is no exception [52,56,60–65]. In fact, Kopper *et al.* successfully generated organoid lines representative of all main subtypes of EOC, along with normal fallopian tube and ovarian surface epithelium [56]. Similarly to what has been reported for all other cancer organoids, OC organoids reproduce the morphological and genetic features of their source tumors, matching typical markers' expression and mutational landscapes [52,56,61–65]. Additionally, these organoids retain intra- and intertumoral heterogeneity, also reflected in the differential sensitivity of each patient's organoid line to chemotherapy and targeted drugs [56,61,65]. This drug response often reflects that of patients', which combined with their relatively fast establishment (usually less than three weeks), highlights their use for drug screening [61,62,65]. All things considered, OC PDTOs thus appear to be a reliable preclinical model for assessing tumor response to treatment and allowing tailored therapy regimens to each individual patient.

2. Project goals

As previously said, survival rates for EOC, particularly HGSOC, are quite low [3,8]. This is partly due to a restricted offer of therapeutic options and a lack of biomarkers for predicting response to treatment [64]. Therapy usually involves the use of platinum-based agents, alone or together with PARPi, yet no tests that accurately predict how each tumor will respond to these therapeutic agents are currently available [64]. Therefore, it is critical to identify predictive biomarkers which will make it possible to characterize tumors' susceptibility to treatment, thus offering the chance for personalized therapeutics [66]. A recent study showed that low expression of *BRCA1/2* mRNA confers platinum-hypersensitivity to ovarian cancers [67]. Since previous clinical studies in recurrent ovarian cancer had evidenced that sensitivity of HGSOC to PARPi might be related to the response to platinum-based therapy [68], the authors speculated that the levels of *BRCA* transcripts might be strong biomarkers to predict cancers' response to PARPi, as well as to other drugs whose effect is linked with sensitivity to platinum-based agents [67]. Based on everything described so far, the main goal of this project was to **generate patient-derived ovarian cancer organoids and further assess their use as a reliable preclinical model for predicting tumors' response to therapy**. In particular, the drug sensitivity profiles of organoids would be compared to patients' clinical response and it would be examined how levels and isoforms of *BRCA1/2* transcripts expressed in the original tumors might correlate with such treatment response patterns and DNA repair activity of organoids. It was anticipated that *BRCA* mRNA may represent a novel predictive biomarker for HGSOC.

3. Material and Methods

3.1. Organoid generation and culture

This study was approved by the ethical committee of CUF Descobertas Hospital, Lisbon, Portugal (Projeto de Estudo/Investigação "OVARY", Reference CE – 026/20 – JMS/is). Tumor and normal fallopian tube samples were collected from consenting patients during surgery at CUF Descobertas Hospital and brought to the laboratory in cold DPBS (grisp, Portugal; catalog number gtc13.0500) after pathological assessment. Processing began within 2 to 3 hours after resection. For generation of ovarian cancer organoids, tumor samples were washed with ice-cold DPBS, then diced to small fragments in basal medium [Advanced DMEM/F-12 (ThermoFisher, United Sates of America (USA); catalog number 12634-010), supplemented with 1X GlutaMax (ThermoFisher, USA; catalog number 35050-061), 1% (v/v) HEPES (ThermoFisher, USA; catalog number 15630-080) and 1% (v/v) Pen-Strep (ThermoFisher, USA; catalog number 15070-063)] using a scalpel. These pieces were poured into pre-warmed (37ºC) basal medium containing Type II Collagenase (ThermoFisher, USA; catalog number 17101-015) to obtain a final concentration of 2.5 mg/mL and incubated for 30 to 45 minutes at 37ºC with shaking. The homogenate was then diluted 1:1 with ice cold basal medium to inactivate the Collagenase and filtered through a 70 µm cell strainer (Corning, USA; product number 352350). Next the cell suspension was spun at 300xg for 10 minutes at 4ºC, the supernatant was discarded, and the pellet washed with 10 mL of ACK Lysing Buffer (ThermoFisher, USA; catalog number A1049201) if red blood cells were present. After a final wash with DPBS, the pellet was resuspended in an appropriate volume of DPBS and a cell count was performed.

For culture, approximately $2.3x10^5$ cells were mixed with 300 µL of phenol-red free Matrigel® (Corning, USA; product number 356237) previously thawed on ice. Droplets of 45 µL of Matrigel (containing approximately 30 000 to 40 000 cells) were placed on a pre-warmed (37ºC) 6-well plate. The plate was left upside down on an incubator at 37ºC for 20 minutes to allow Matrigel to solidify, then 2 mL of tumor organoid complete medium was added. Tumor organoid complete medium is Advanced DMEM/F-12, supplemented with 1X GlutaMax, 1% (v/v) HEPES, 1% (v/v) Pen-Strep, 100 ng/mL Noggin (Peprotech, USA; catalog number 120-10C), 100 ng/mL R-Spondin1 (Peprotech, USA; catalog number 120-38), 1X B27 (ThermoFisher, USA; catalog number 17504-044) 1.25 mM N-Acetyl-L-Cysteine (Sigma, USA; catalog number A9165), 10 mM Nicotinamide (Sigma, USA; catalog number N0636-100G), 5 µM A83-01 (Sigma, USA; catalog number SML0788), 100 ng/mL FGF-10 (Peprotech, USA; catalog number 100-26), 100 ng/mL EGF (Peprotech, USA; catalog number AF-100-15), 10 ng/mL FGF-2 (Peprotech, USA; catalog number 100-18B), 1 µM Prostaglandin E2 (Tocris, United Kingdom (UK); catalog number 2296/10) and 10 µM SB 202190 (Sigma, USA; catalog number S7076). 10 µM ROCK inhibitor Y-27632 (StemCell Technologies, Canada; catalog number 72304) is added to the complete medium upon initial plating of cells, then removed when medium is changed. Medium was changed every 2-3 days.

For generation of normal fallopian tube organoids, samples were also washed with ice-cold DPBS and then cut into small sections in pre-warmed digestion buffer [Basal medium containing 0.5 mg/mL DNase I (Sigma, USA; catalog number 10104159001), 2 mg/mL Trypsin from bovine pancreas (Sigma, USA; catalog number T9935) and 0.5 mg/mL Type II Collagenase (ThermoFisher, USA; catalog number 17101-015)] using scissors. This homogenate was incubated for 45 minutes at 37ºC with shaking, then filtered and spun similarly to tumor samples. The pellet obtained was washed with DPBS, resuspended in approximately 30 µL of DPBS and then mixed with 300 µL of Matrigel. The following steps were as described previously for generation of cancer organoids, except complete medium was additionally supplemented with 25% (v/v) Wnt-3A conditioned medium, R-Spondin1 was at a final concentration of 500 ng/mL, and it did not contain FGF-2, Prostaglandin E2 nor SB 202190.

When deemed necessary (usually once a week), organoids were passaged at suitable ratios (typically between 1:1 to 1:3, depending on organoid confluency). For passaging, organoids were incubated with 1 mL of pre-warmed (37ºC) Accutase® solution (Sigma, USA; catalog number A6964), for up to 5 minutes at room temperature, then mechanically sheared through a P1000 pipet tip connected to a P200 pipet tip without filter and transferred to a Falcon® tube with 10 mL of cold basal medium. Organoid fragments were collected by centrifugation at 300xg for 10 minutes at 4ºC, resuspended in the appropriate volume of basal medium and mixed with Matrigel for reseeding as above.

Organoid cultures were observed on a Zeiss Primovert bright-field inverted microscope, using 4x and 20x objectives, every 2-3 days and images were captured using a Zeiss AxioCam ERc5s camera.

3.2. Production of Wnt-3A conditioned medium

Wnt-3A conditioned medium was produced in-house by culturing L Wnt-3A (ATCC® CRL-2647™) cells according to the supplier's instructions. Briefly, after initial culture in complete growth medium [DMEM (ThermoFisher, USA, catalog number 41966-029), supplemented with 10% (v/v) FBS (ThermoFisher, USA; catalog number 10270-106) and 0.4 mg/mL G-418 (Calbiochem, USA; catalog number 345810)], cells were split 1:10 in 10 mL of culture medium without G-418, in 75 cm^2 flasks, and grown for 4 days. Then medium was removed and sterile filtered with low protein binding, 0.22 µm filter units (Merck, Germany; catalog number SLGVV255F) making the first batch of conditioned medium. After addition of 10 mL of fresh medium to the flask and culture for another 3 days, medium was removed and sterile filtered, making the second batch of conditioned medium. To make the Wnt-3A conditioned medium, the first and second batches were mixed 1:1. Cells were discarded at this point due to being overgrown.

3.3. Immunofluorescence of whole-mount organoids

Upon organoid passaging, two Matrigel droplets of 10 µL were plated in each well of a µ-Slide 8 Well chambered coverslip (ibidi, Germany; catalog number 80826) and covered with 200 µL of complete medium. Once ready for fixation, medium was removed, the wells were rinsed with 1x PBS, 300 µL of 4% (w/v) PFA (Sigma, USA; catalog number P6148) in 1x PBS was added to each well and the organoids were fixed for 20 minutes, at room temperature, with gentle swirling. Then each well was washed with 300 µL of 1x PBS, three times for 10 minutes each and organoids were stored in 1x PBS at 4ºC until proceeding for permeabilization. For permeabilization, PBS was removed and 300 µL of 0.5% (w/v) Triton™ X-100 (Sigma, USA; catalog number T9284) in 1x PBS was added to each well, for 20 minutes, at room temperature, with gentle swirling. Wells were then washed three times for 5 minutes each with 300 µL of 1x PBS. Blocking was done by incubating the organoids with 150 µL of 3% (w/v) BSA (Sigma, USA; catalog number A2153) in 1x PBS, for 45 minutes at room temperature. Primary antibodies used were rabbit anti-Ki67 (abcam, UK; catalog number ab833) at 1/100 and mouse anti-EpCAM conjugated with FITC (abcam, UK; catalog number ab8666) at 5 µg/mL (2.5/100). Antibodies were diluted in 1.5% (w/v) BSA in 1x PBS and the wells were incubated with 150 µL of the respective antibodies, in a dark humid chamber, overnight at 4ºC. The next day each well was rinsed twice, then washed three times for 10 minutes each with 1x PBS containing 0.05% Tween® 20 (Sigma, USA; catalog number P1379). Secondary antibodies used were horse anti-mouse IgG DyLight® 488 (Vector Laboratories, USA; catalog number DI-2488) at 1/100 and goat anti-rabbit IgG DyLight® 594 (Vector Laboratories, USA; catalog number DI-1594) at 1/100, both from a 1:1 stock in glycerol. These were also diluted in 1.5% (w/v) BSA in 1x PBS and the wells were incubated with 150 µL of the respective antibody, in the dark, for 1 hour at room temperature. Then, wells were rinsed twice and washed for 10 minutes with 300 µL of 1x PBS containing 0.05% Tween® 20, followed by a 10 minute incubation with 300 µL of 0.5 µg/mL DAPI in 1x PBS. The organoids were then washed three times for 5 minutes each with 300 µL of 1x PBS containing 0.05% Tween® 20. After the final wash, 100 µL of

mounting medium made in-house was added to each well and the stained organoids were stored at 4ºC in the dark until microscopic analysis. Mounting medium is 9.2 mM p-Phenylenediamine (Sigma, USA; catalog number 695106) in 90% (w/v) sterile glycerol (Sigma, USA; catalog number G6279) and 1x PBS, pH 9.5. Images were acquired on a Zeiss LSM 710 confocal point-scanning microscope using the Plan-Apochromat 20x/0.8 M27 objective. Dylight® 488 fluorescence was detected using the 488 nm line of the argon ion laser. Dylight® 594 was excited with the DPSS 561-10 laser and DAPI fluorescence was detected using the Diode 405-30 laser. Each channel was recorded independently and pseudocolor images were generated and superimposed.

3.4. Immunohistochemistry of organoids

When ready for organoid fixation, medium was removed, and wells were washed with 1x PBS. Two fixation protocols were successfully used. In the first protocol, 2 mL of 4% PFA in PBS was added to the wells and organoids were incubated at room temperature for 45 minutes with gentle swirling. Then they were transferred to a 15 mL Falcon® tube with a plastic Pasteur pipette and let to settle at the bottom for another 15 minutes. PFA was removed and 8-10 mL of formalin (Bio-Optica, Italy; product number 05-01005Q) was added. In the second protocol, formalin was added directly to the wells, organoids were transferred to a 15 mL Falcon® tube with a plastic Pasteur pipette and more formalin was added to a final volume of 8-10 mL. In both cases, fixated organoids were left at room temperature until further processing. No changes were detected between organoids fixated with different protocols.

Histological analysis was done at the pathology department of CUF Descobertas Hospital. There, fixated organoids were spun down to a pellet and resuspended in warm HistoGel™ (ThermoFisher, USA; catalog number HG-4000-012). The mixture was solidified at 4ºC for 5-10 minutes, then processed and paraffin-embedded, cut to 3µm sections on positively charged slides, and then stained with Hematoxylin & Eosin or processed for immunohistochemistry (IHC) with PAX-8, WT1, p53, or Ki67 antibodies as described next. All IHC was performed on the Ventana BenchMark ULTRA automated staining platform. All antibodies were pre-diluted and run using the OptiView DAB IHC Detection Kit (Roche, Switzerland; catalog number 760-700) with ULTRA CC1 antigen retrieval (Roche, Switzerland; catalog number 950-224). Antibodies used were PAX-8, clone MRQ-50 (Cell Marque, USA; catalog number 760-4618), WT1, clone 6F-H2 (Roche, Switzerland; catalog number 760-4397), p53, clone DO-7 (Roche, Switzerland; catalog number 800-2912) and Ki67, clone 30-9 (Roche, Switzerland; catalog number 790-4286).

3.5. Drug sensitivity assay

Upon organoid passaging, 10 µL droplets were plated in each well of a black, clear flat bottom 96-well plate (Tecan, Switzerland; catalog number 30122306) and covered with 100 µL of complete medium. After two days, medium was changed to complete medium containing either olaparib (Santa Cruz Biotechnology, USA; catalog number sc-302017), cisplatin (Sigma, USA; catalog number 232120-50MG) or carboplatin (Sigma, USA; catalog number C2538) at different concentrations. After 5 days in culture with drugs, an equal volume of CellTiter-Glo® (Promega, USA; catalog number G7570/G7571) was added to each well and the luminescence was read on a TECAN microplate reader (TECAN Infinite M200). The drug concentrations used were as follows: olaparib at 0 µM (contained Milli-Q® H_2O at a volume equal to the volume used in the highest olaparib dose), 0.05 µM, 0.5µM, 1 µM, 10 µM, 25 µM and 50 µM; cisplatin at 0 µM (contained DMSO at a volume equal to the volume used in the highest cisplatin dose), 1 µM, 2 µM, 5 µM, 20 µM, 50 µM and 100 µM; carboplatin at 0 µM (contained Milli-Q® H_2O at a volume equal to the volume used in the highest carboplatin dose), 5 µM, 10 µM, 25 µM, 50 µM and 75 µM. IC50s were calculated using GraphPad Prism 8 (Nonlinear regression, [Inhibitor] vs response (three parameters)).

4. Results

The main aim of this project was to generate organoids from EOC, in particular high-grade serous carcinoma, to evaluate their use as a model for predicting the response of tumors to treatment. We started by the optimization of a protocol for organoid derivation and culture, however due to a lack of samples after this protocol was optimized, we were only able to successfully derive organoids from a low-grade serous tumor and normal fallopian tubes. These organoids were morphologically characterized and drug sensitivity assays were implemented.

4.1. Successful generation of patient-derived LGSOC and normal fallopian tube organoids

Since the patient-derived organoid technology was not yet implemented in the host laboratory, a protocol for organoid generation and culture had to be optimized. Cancer and normal (unmatched) fallopian tube (FT) tissue was obtained from consenting patients undergoing tumor resection or hysterectomy and bilateral salpingo-oophorectomy, respectively, and used for organoid derivation and histological analysis. Samples were collected from different types of EOC, namely high-grade serous, mucinous, serous borderline, endometrioid, clear-cell, and low-grade serous, but only this last one successfully originated an organoid line. For tissue dissociation and general culture medium conditions, we followed the work described by Hill *et al.* [64]. Based on previous experience from the host laboratory in generating cerebellar organoids from human induced pluripotent stem cells, we initially started by seeding the dissociated tumor cells in AggreWell™ plates (StemCell Technologies). However, this method was unsuitable for the growth of tumor-derived organoids since, upon cell seeding, we only observed the formation of sphere-like structures that showed no changes in growth over time, and when transferred to ultra-low attachment plates eventually dissociated. Therefore, we then decided to culture the tumor cells in Matrigel, a substitute of extracellular matrix commonly used for growing organoids [69,70]. Using this method for seeding cells, organoids initially formed for some of the samples received but their derivation efficiency was low and most cultures could not be maintained after the first passage. Nonetheless, with the optimized culture protocol (Fig. 4.1), we managed to establish organoids from a LGSOC which were passaged 7 times and expanded for 65 days (Fig. 4.2, bottom panel). We also established two organoid lines from normal FT (Fig. 4.2, top panel) intended to be used as controls for the drug sensitivity assays of tumor organoids. The first FT organoids were passaged 10 times and expanded for 73 days, while the second were passaged 8 times and expanded for 58 days.

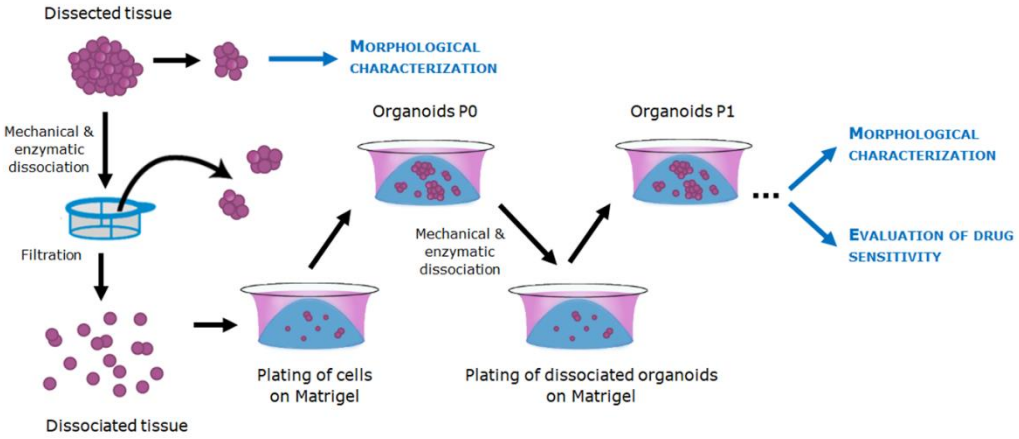

Figure 4.1 | Overview of the organoid culture protocol. Tumor and FT samples are collected during surgery. A piece is used for morphological characterization. For organoid generation, tissue is mechanically and enzymatically dissociated (type II collagenase for tumors and a cocktail of type II collagenase, trypsin from bovine pancreas and DNase I for FT). Cell suspensions are filtered and centrifuged, and cells are resuspended in Matrigel and plated. (continues on the next page)

Once ready for passaging, organoids are dissociated from Matrigel with Accutase® solution and mechanically sheared through a P1000 pipet tip connected to a P200 pipet tip without filter. Organoid fragments are collected by centrifugation, resuspended in the appropriate volume of medium and reseeded in Matrigel as for initial culture Organoid cultures are morphologically characterized and their sensitivity to drugs is evaluated.

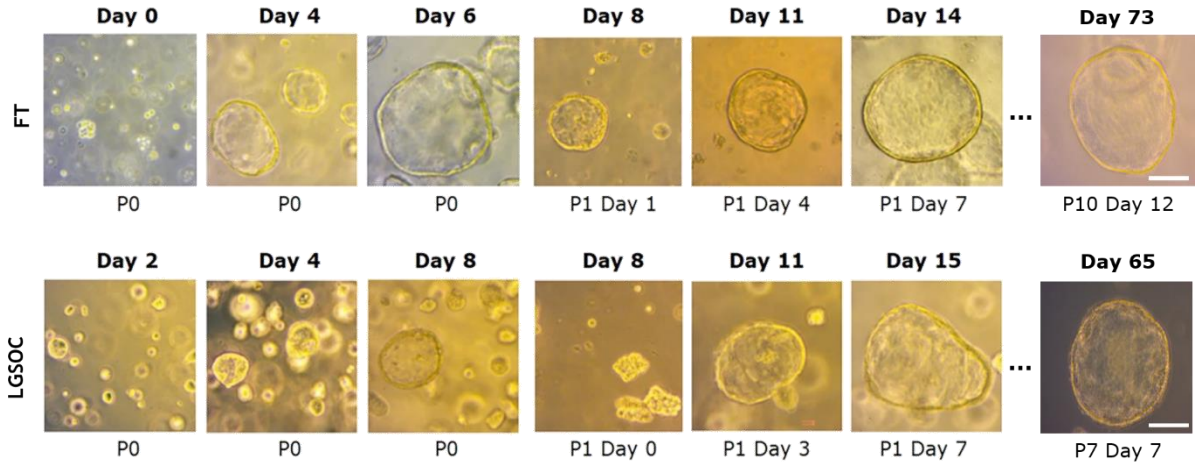

Figure 4.2 | Representative bright-field images of patient-derived organoids in the first two weeks and the last day of culture. First organoid line of normal fallopian tube - FT (top) and low-grade serous ovarian carcinoma - LGSOC (bottom). There were no major morphological differences between FT organoid lines. Scale bar, 100 μm.

During establishment of tumor organoid cultures, three culture medium conditions were tested: condition A was the complete medium (described in the Material and Methods section), condition B did not contain Noggin and condition C did not contain Noggin nor R-Spondin1. We decided to test different growth conditions after Hoffman *et al.* [63] reported that Noggin seemed to be detrimental for the expansion of HGSOC organoids, while only a few cultures benefited from the addition of R-Spondin1. When we first initiated a culture of LGSOC organoids, those growing in condition A appeared to have a faster growth rate than the ones in the other conditions, revealed by the fact the culture reached confluency 2 days before (7 days vs 9 days). After 3 passages, growth rates of all conditions seemed to equal, but following passage 4 all organoids started showing signs of cell death (individual cells on the surface and around the organoids, and darkened structures), particularly the ones in condition C, so they were concentrated rather than expanded on passage 5. After this passage organoids recovered, growing in size and number, however, after 6 passages organoids in condition C appeared to grow less, with a lower density than the remaining conditions, and were no longer passaged after 53 days in culture. This suggests that R-Spondin1 may be required for longer-term expansion of LGSOC organoids. Conditions A and B were passaged one more time and expanded until they seemed not to grow further. Culture of LGSOC organoids was discontinued after 65 days. Between conditions A and B, organoids seemed to proliferate slightly more on the latter, especially after passage 4, but the difference in growth was not clear. This might indicate that the presence of Noggin does not affect the expansion of LGSOC and may even be beneficial. Organoid morphologies did not seem to vary between different medium conditions when observed on a bright-field microscope, suggesting the presence or absence of the components tested does not affect organoid structure.

As for FT, organoid generation was successful with both samples received. Organoids derived from the first sample (FT-1) were observed after just 2 days in culture. Following passage 2, on day 15, their growth rate greatly increased, with the cultures always showing elevated densities, and some passages having to be performed twice a week. After 10 passages, however, organoids seemed to stop growing and the culture was discontinued on day 73. Organoids derived from the second sample (FT-2) had a very slow growth rate in the beginning, with only a few visible organoids after 5 days in culture;

organoids only grew in size but not in number. Therefore, they were concentrated rather than expanded on the first passage, on day 11, and their growth increased, especially number-wise. Like FT-1, from passage 2 on, organoid cultures became confluent very fast, sometimes having to be passaged twice a week. On passage 6, some organoids showed signs of cell death and density became considerably lower, allowing organoids to grow in size. On passage 7 organoid density remained low and there was a clear heterogeneity in organoid size, as well as several organoids showing signs of cell death. Following passage 8, however, organoids did not seem to recover and the culture was discontinued after 58 days. Bright-field microscopy imaging did not reveal any major differences in morphology between FT-1 and FT-2 organoids.

Even though efficiency was low, we were able to establish a protocol for organoid generation and culture, having successfully derived ovarian cancer organoids, along with normal fallopian tube organoids, thus implementing this technology in the host laboratory.

4.2. Patient-derived LGSOC and normal FT organoids histologically recapitulate their tissue of origin

In order to evaluate whether the organoids we generated resembled either the parent tumor or the parent healthy tissue, a hematoxylin and eosin (H&E) staining was performed and an immunohistochemical (IHC) analysis was done with a typical marker panel used in the clinical setting.

Morphologic characterization of the LGSOC organoids using standard H&E staining revealed globally spherical structures with cribriform architecture (Fig. 4.3, Organoids H&E staining), a feature of complexity, and micropapillary projections (Appendix, Fig. 8.1, right panel), a highly specific feature for LGSOC. Epithelium is predominantly multi-layered, with disorganization, being composed of small cubic to columnar cells, with low nuclear pleomorphism. Rare mitotic figures were observed. These characteristics are in line with the cytology expected for this type of tumor. At different timepoints during culture, organoids were found in distinct stages of maturation, with differences in size and differentiation (Appendix, Fig. 8.1). IHC analysis also revealed a match between the LGSOC organoids and the tumor from which they were derived (Fig. 4.3). Both the tumor and the organoids stained positive for the Müllerian marker PAX8, and for WT1, a marker for the serous subtype of ovarian carcinomas. The LGSOC organoids exhibited a wild-type p53 staining pattern, as is normally present in these tumors.

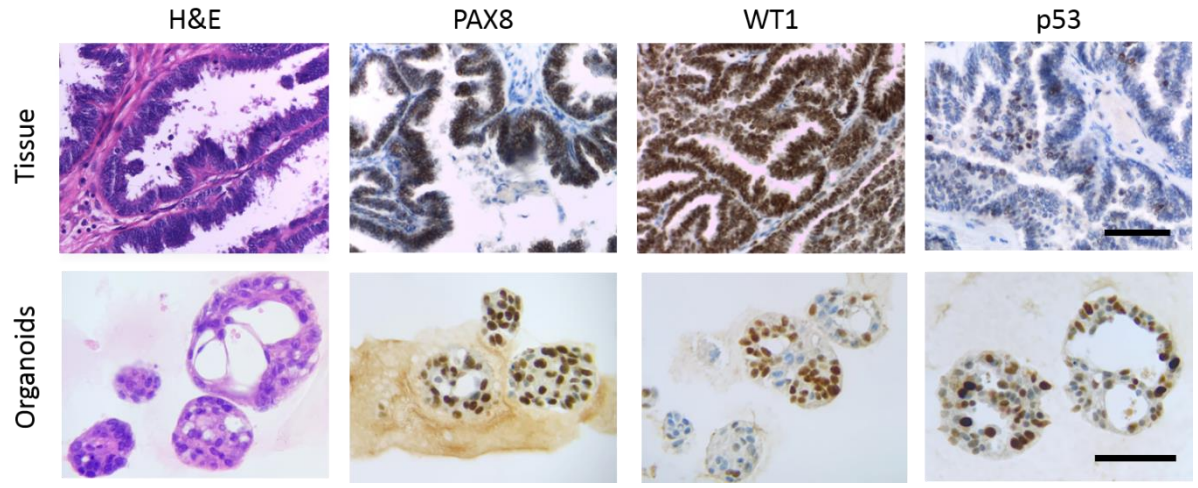

Figure 4.3 | Low-grade serous ovarian carcinoma (LGSOC) organoids histologically mimic the parent tumors from which they were derived. Histological comparison of representative LGSOC organoids (bottom) to their corresponding tumor tissue (top) by H&E staining (first panel on the left), PAX8 staining (second panel on the left), WT1 staining (second panel on the right) and p53 staining (first panel on the right). Organoids maintain positive PAX8 and WT1 staining and p53 wild-type pattern. Scale bar, 100 µm.

Morphologic characterization of the FT organoids using the same methodology as for LGSOC, revealed spherical structures composed of a monolayered epithelium with highly polarized cubic to columnar cells, with basal nuclei and the apical pole oriented to the luminal side (Fig. 4.4, Organoids H&E staining). Occasional mitotic figures were detected (Appendix, Fig. 8.2, double arrow). Both secretory and ciliated cells (Appendix, Fig. 8.2, arrow) were present. The development of epithelium folds was also identified in several organoids (Appendix, Fig. 8.2, right panel), recapitulating an important feature present in normal human fallopian tube. FT organoids also matched their tissue of origin, as revealed by the IHC analysis (Fig. 4.4). Both the organoids and the parent FT tissue show strong and diffuse expression of PAX8 (a secretory cell marker), and exhibit a wild-type p53 staining pattern. However, expression of WT1 (usually present in epithelial cells of the fallopian tube and ovary) was unexpectedly weaker in the FT organoids. Organoids display a much higher proliferative index than the original tissue, represented by the number of Ki-67-positive cells.

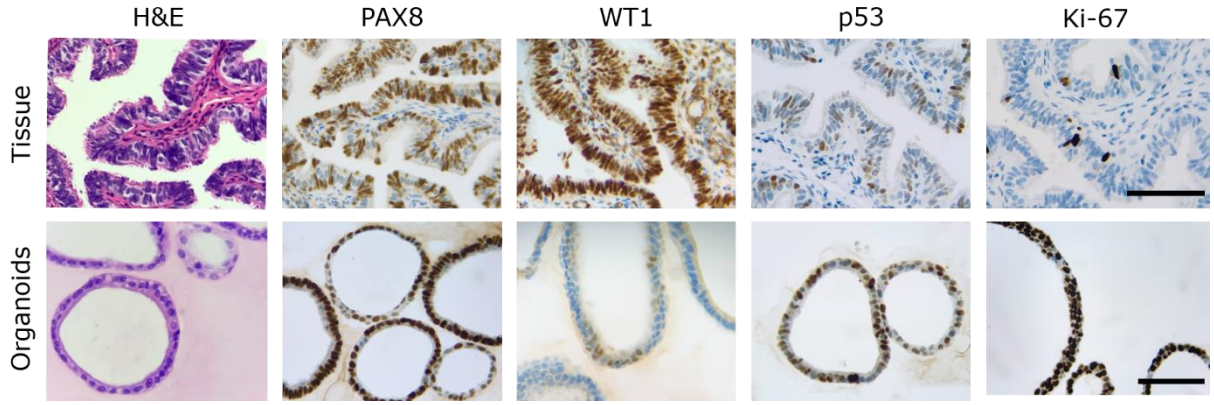

Figure 4.4 | Fallopian tube (FT) organoids histologically mimic the parent tissue from which they were derived. Histological comparison of representative healthy FT organoids (bottom) to their corresponding tissue (top) by H&E staining (first panel on the left), PAX8 staining (second panel on the left), WT1 staining (middle panel) and p53 staining (second panel on the right). The proliferation index was also evaluated by Ki-67 staining, revealing a higher proliferation of organoids (first panel on the right). Organoids maintain positive PAX8 staining and p53 wild-type pattern but show a weaker WT1 staining. Scale bar, 100 µm.

Taken together, these results indicate that patient-derived low-grade serous ovarian cancer and fallopian tube organoids retain most of the histological features of the tissue from which they were derived, diseased and healthy, respectively.

4.3. Immunofluorescent staining reveals distinct morphologies and proliferation rates between patient-derived LGSOC organoids and normal FT organoids

To better understand the structural organization of the patient-derived organoids, we decided to perform an immunofluorescence (IF) analysis, using epithelial cell adhesion molecule (EpCAM) to visualize cell membranes and DAPI to visualize nuclei. It became clear that tumor organoids and FT organoids have strikingly distinct morphologies. Similarly to human fallopian tubes, FT organoids formed hollow structures with a well-oriented epithelium (Fig. 4.5, A). LGSOC organoids, on the other hand, formed denser and more complex structures harboring multiple lumens that resemble solid tumor masses (Fig. 4.5, B).

Seeing that FT organoids displayed a faster growth than LGSOC organoids, we decided to look for differences in cell proliferation using the Ki-67 nuclear marker. Indeed, there was a higher proportion of proliferating cells in FT organoids when compared to tumor organoids (Fig. 4.6).

Collectively, these results further demonstrate that low-grade serous carcinoma organoids are very different from healthy fallopian tube organoids, not only in terms of cellular architecture but also in their ability to proliferate, with normal organoids showing higher growth rates than tumor organoids.

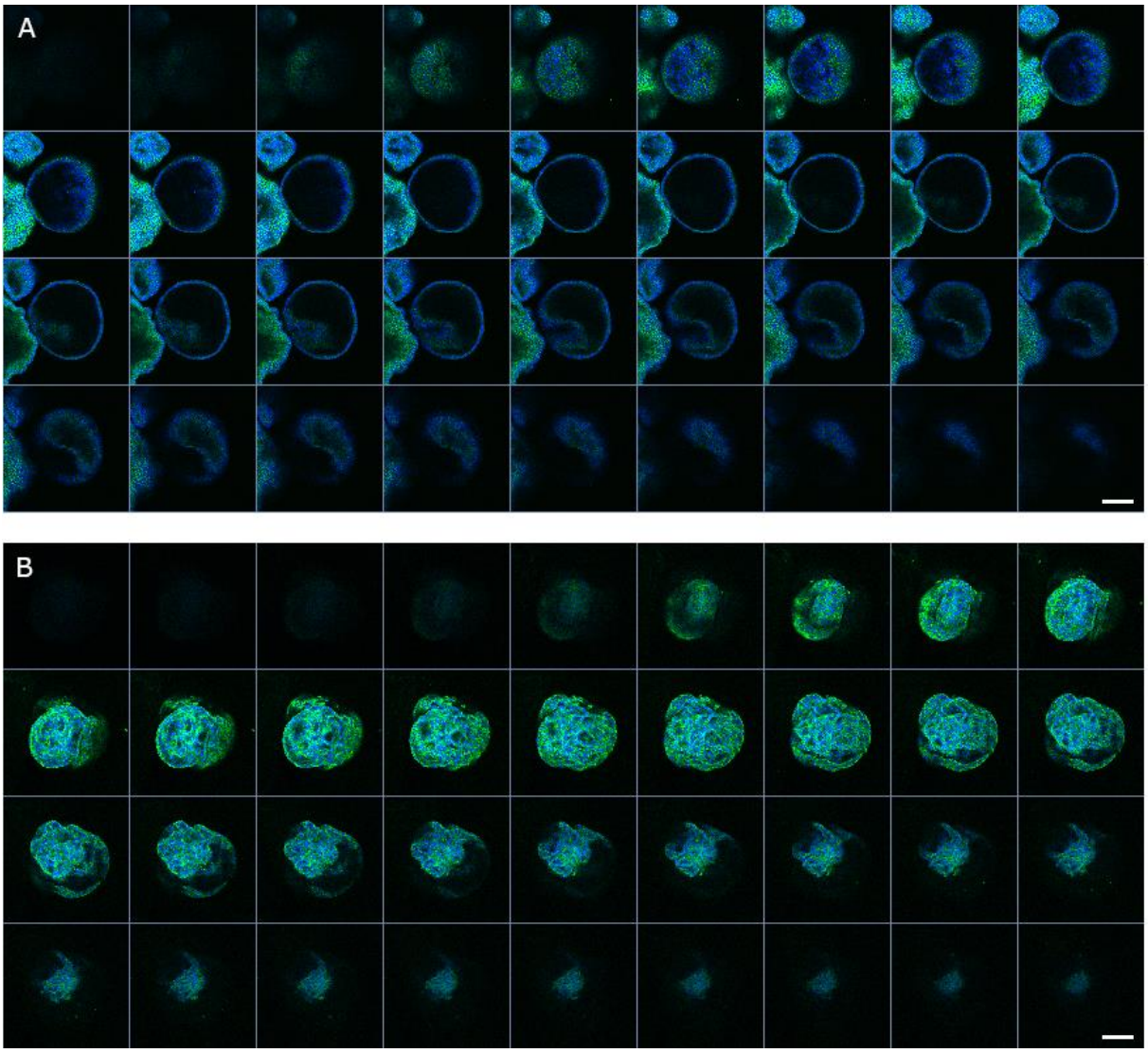

Figure 4.5 | Immunofluorescent staining of whole-mount patient-derived fallopian tube - FT (A) and low-grade serous ovarian carcinoma - LGSOC (B) organoids reveals clear morphological differences between both organoids. Organoids were stained for the epithelial marker EpCAM (green) and nuclear marker DAPI (blue). FT organoids appear as hollow structures with a well-oriented epithelium whereas LGSOC organoids formed denser and more complex structures harboring multiple lumens. Scale bar, 100 µm.

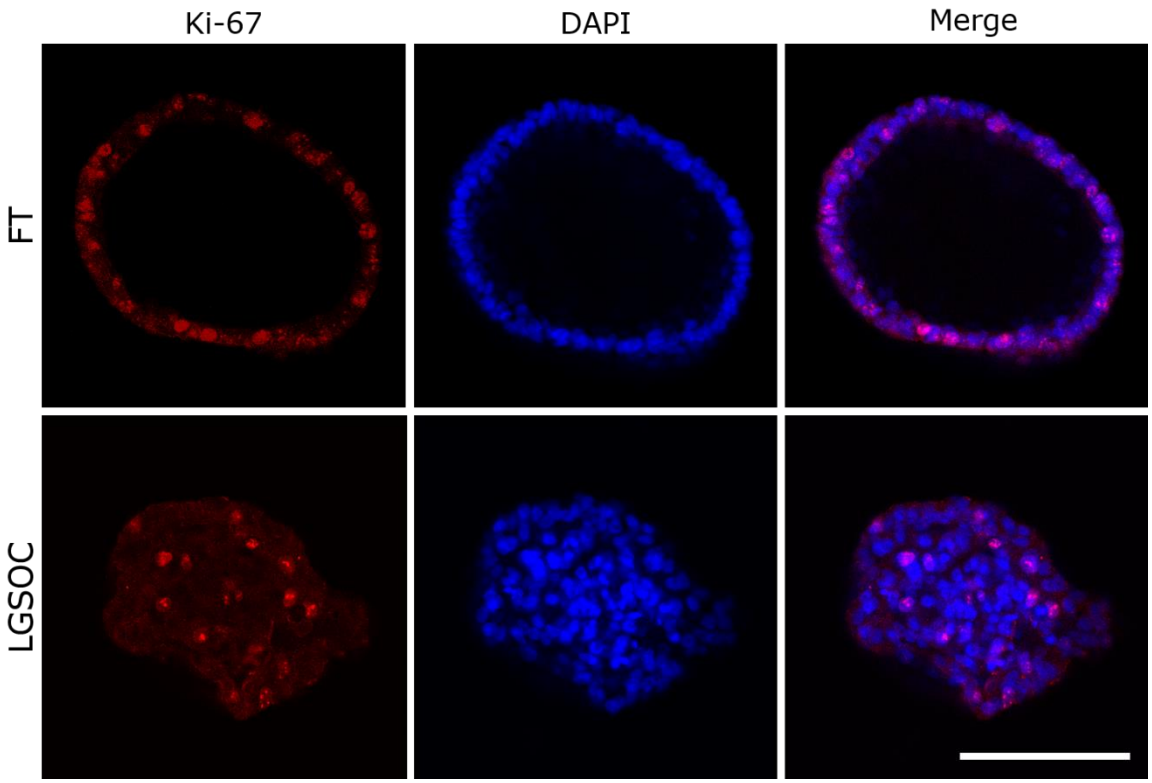

Figure 4.6 | Immunofluorescent staining of whole-mount patient-derived fallopian tube - FT (top) and low-grade serous ovarian carcinoma - LGSOC (bottom) organoids using proliferation marker Ki-67 reveals proliferative differences between both organoids. Organoids were stained for the proliferation marker Ki-67 (red) and nuclear marker DAPI (blue). FT organoids display a higher proportion of proliferating cells when compared to LGSOC organoids. Scale bar, 100 μm.

4.4. LGSOC organoids lack therapeutic sensitivity to chemotherapy and PARP inhibition while FT organoids appear to be sensitive to elevated doses of platinum-based drugs

The main goal of this project was to evaluate the use of patient-derived tumor organoids as a platform to predict tumor's response to therapy in the clinical setting. Therefore, drug sensitivity assays were performed on the LGSOC organoids we generated, as well as on the FT ones as healthy controls. This was assessed by measuring cell viability using the CellTiter-Glo® Luminescent Cell Viability Assay (Promega, USA). This reagent allows for the determination of the number of viable cells in culture based on quantitation of the ATP present, an indicator of metabolically active cells; the luminescent signal generated after cell lysis is proportional to the amount of ATP present, which in turn is directly proportional to the number of viable cells [71].

We started by testing organoids' response to the platinum-based drug cisplatin and to the PARP inhibitor olaparib. The tumor organoids did not appear to be sensitive to cisplatin (Fig. 4.7, A), nor to olaparib (Fig. 4.7, B). On the other hand, both FT organoid lines displayed a high sensitivity to elevated doses of cisplatin (Fig. 4.8, A), but, alike LGSOC organoids, no effect was observed with olaparib (Fig. 4.8, C). Since cisplatin appeared to be highly toxic to healthy tissue at high concentrations, we tested the organoids' response to carboplatin, the platinum-based agent used in standard-of-care treatment for ovarian cancer. However, by the time this drug became available, LGSOC organoids were no longer in culture and we were only able to test its effect on FT organoids. These did not seem to be sensitive to carboplatin (Fig. 4.8, B) since viability was only affected at high concentrations of the drug and to a much less extent than cisplatin.

Overall, these results suggest that the viability of both LGSOC and FT organoids is not affected by inhibition of PARP. Moreover, high doses of cisplatin seem to be lethal to FT organoids, but not to LGSOC, whereas carboplatin appears to be less toxic.

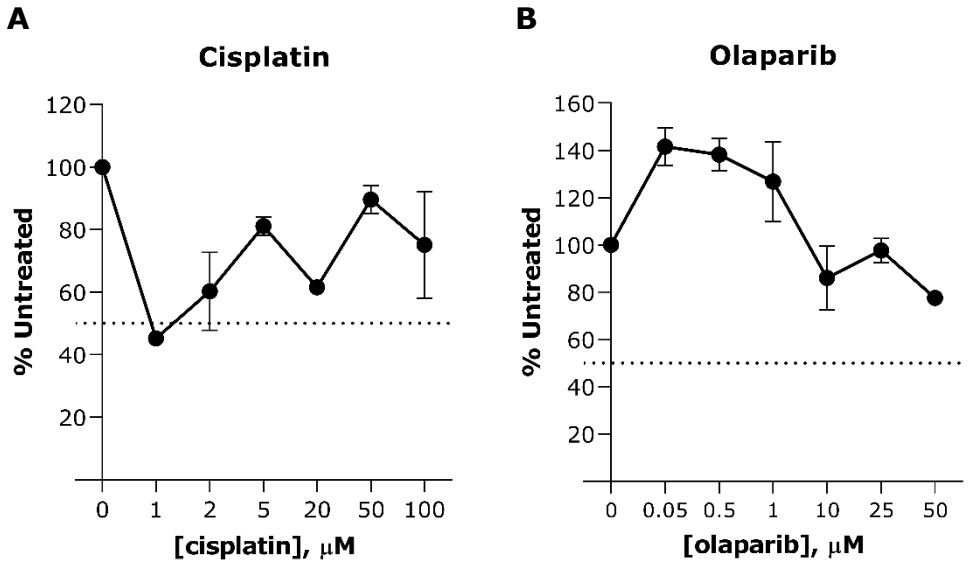

Figure 4.7 | Low-grade serous ovarian carcinoma (LGSOC) organoids lack therapeutic sensitivity to cisplatin and to the PARPi olaparib. Sensitivity dose curves of an LGSOC organoid line (passage 2) to cisplatin (**A**) and olaparib (**B**). A dashed line marks 50% untreated. Dots represent the mean of technical duplicates and error bars represent SD of technical duplicates. IC50 for olaparib = 70.97 μM.

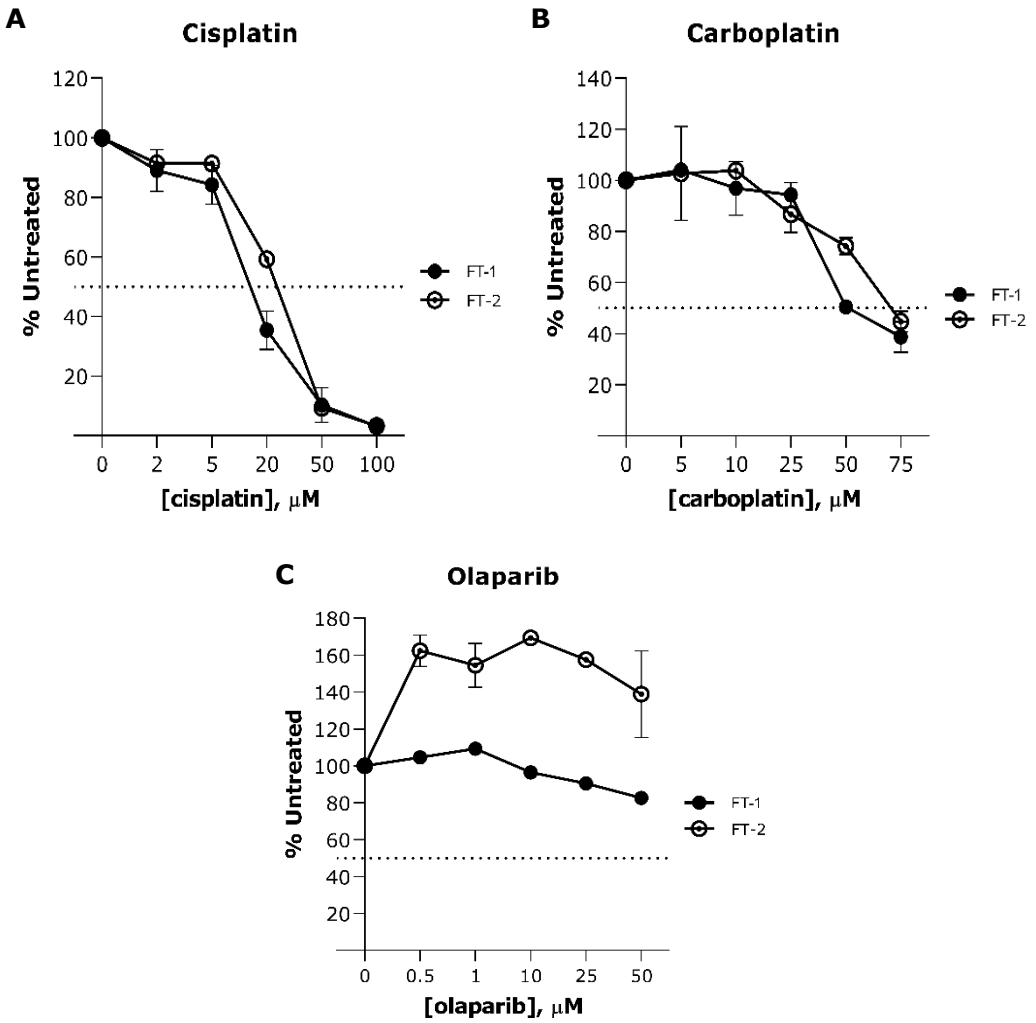

Figure 4.8 | Fallopian tube (FT) organoids lack therapeutic sensitivity to the PARPi olaparib. Elevated concentrations of cisplatin are lethal to FT organoids whereas carboplatin seems to be less toxic. Sensitivity dose curves of two FT organoid lines to cisplatin (**A**), carboplatin (**B**) and olaparib (**C**). A dashed line marks 50% untreated. Assays were performed on passage 6 and 10 of FT-1, and on passage 4 of FT-2. **A,** For FT-1, dots represent the mean of biological duplicates and error bars represent SD of biological duplicates. For FT-2, dots represent the mean of technical duplicates and error bars represent SD of technical duplicates. **B and C,** Dots represent the mean of technical duplicates and error bars represent SD of technical duplicates. IC50 of FT-1 for olaparib = 179.70 μM. IC50 for cisplatin = 11.18 μM and 16.48 μM for FT-1 and FT-2, respectively. IC50 for carboplatin = 58.15 μM and 82.83 μM for FT-1 and FT-2, respectively.

5. Discussion

Ovarian cancer represents the second leading cause of gynecologic cancer-associated death [1]. Epithelial ovarian cancer (EOC) is the most predominant type of this group of heterogenous diseases, and the histological subtype of serous carcinomas comprises the majority of malignant EOC [5]. These can be further subdivided into high-grade serous ovarian carcinoma (HGSOC) and low-grade serous ovarian carcinoma (LGSOC), but the two are very distinct diseases, with differences in histology, genomic alterations and treatment response [2]. HGSOC makes up 90% of all cases of serous carcinomas and survival rates are quite low, with most patients being diagnosed at late stages, in part due to a limited offer of therapeutic options and a lack of biomarkers for predicting treatment response [3,64]. Therapy usually involves the use of platinum-based agents, alone or in combination with PARPi, however it remains crucial to identify predictive biomarkers which will allow for a characterization of individual tumors' susceptibility to such drug regimens [64,66]. Recently, patient-derived cancer organoids have emerged as potential *in vitro* models that faithfully recapitulate the original tumors [56,64]. These are three-dimensional cell cultures derived from primary tumor cells that can mimic physiological and anatomical features, as well as the functionality of parental tumors [55,64,72], and provide an improved platform for prediction of therapeutic responses in cancer patients over more commonly used tumor models [51,58]. This project was thus aimed at generating patient-derived ovarian cancer organoids to assess their use as a reliable preclinical model for predicting tumors' response to therapy. By comparing organoids' drug sensitivity profile to patients' clinical response, and correlating their response patterns to *BRCA* expression, we hypothesized that *BRCA* transcripts may function as a biomarker for predicting drug response in HGSOC.

We started by the optimization of a protocol for generating and culturing patient-derived organoids, as this technology was yet to be implemented in the host laboratory. For sample processing and culture medium conditions we followed the procedure described by Hill *et al.* [64], but initially opted for a different way of seeding cells. Based on previous experience from the host laboratory in generating cerebellar organoids from human induced pluripotent stem cells, we used AggreWell™ plates (StemCell Technologies). After failed attempts at deriving organoids from the first few ovarian cancer samples, which included the only HGSOC samples received, we concluded this method was not suitable for growing tumor-derived organoids. AggreWell™ plates are usually used to generate spheroids [73] which are three-dimensional cultures that result from the simple aggregation of cells in a scaffold-free manner. Organoids, on the other hand, form from the differentiation of stem cells in a matrix-based environment. [74,75]. The failure at developing tumor organoids on AggreWell™ plates further supports the notion that these organoids also require a scaffold for their development [47,76]. The majority of studies describe the culture of organoids on a substitute of extracellular matrix (ECM), usually Matrigel (Corning) or Basement Membrane Extract (BME) (Cultrex) [70,76]. These matrices are solubilized basement membrane preparations extracted from the Engelbreth-Holm-Swarm (EHS) mouse sarcoma, a tumor rich in ECM proteins and several growth factors [77]. In fact, once we began seeding cells in Matrigel we were able to derive organoids from a low-grade serous ovarian carcinoma. However, for the remaining ovarian cancer samples we received (mucinous, serous borderline, endometrioid and clear-cell), the efficiency of derivation was low and cultures could not be maintained after the first passage because the organoids did not grow back. Spatial proximity between organoids often promotes their growth [78] so it could be that the organoid density was too low. Another possibility was that, when split, the organoids were broken up too small, which has been reported as a factor leading to reduced efficiency of organoid formation [79].

The key aspect of developing organoids is defining the right cocktail of growth factors to supplement culture media, something that differs based on the tissue of origin [58,80]. As mentioned before, when we finally succeeded in establishing and maintaining an organoid culture derived from a LGSOC, we

tested the possible influence of different growth medium conditions on organoid development, based on reports from Hoffman *et al.* [63] for HGSOC. Contrary to Hoffman's observations for HGSOC organoids, our tumor organoids growing in medium without R-Spondin1 and Noggin lost some ability to proliferate before organoids growing in the presence of these factors, which suggests their requirement for long-term culture of LGSOC organoids. R-Spondin1 is an activator of the Wnt/β-catenin signaling pathway, while Noggin inhibits BMP signaling [81]. Both factors have been described as necessary for maintaining stem cell niches [69], hence being usual components of most organoid culture mediums, including ovarian cancer and normal fallopian tube [56,64,82]. Removing Noggin from the culture medium, while keeping R-Spondin1, seemed to slightly increase organoid proliferation at certain passages, but the differences were not pronounced and organoids seemed to develop at similar rates. Taken together these results support the use of Noggin and R-Spondin1 in culture medium for organoids of low-grade serous ovarian carcinoma.

One of the main features of tumor-derived organoids is their ability to recapitulate several characteristics of their parent tumors, including morphology and protein expression profiles [83]. In line with previous reports [56], histological analysis of our LGSOC organoids revealed a match between them and the tumor from which they were derived. Tumor organoids retained expression of WT1 and PAX8, typical markers for the serous subtype of EOC [16], and showed a wild-type pattern for p53, as is normal in low-grade tumors [15]. Similar results were obtained with normal FT organoids, which also mimicked their parent tissue. Unexpectedly, these organoids consistently showed a weaker staining of WT1 when compared to the original tissue. It is possible that the medium in which the organoids were cultured is affecting WT1 expression, but additional research needs to be performed to understand such loss of WT1 staining.

When observed under a bright-field microscope, LGSOC organoids presented morphological differences from FT organoids. Therefore, we decided to take a closer look at their structural organization by performing an immunofluorescent staining for an epithelial cell membrane marker (EpCAM) and a nuclear marker (DAPI). Surely, it was evident that both organoid lines exhibited distinct spatial architectures, with FT organoids appearing as hollow structures with a well-oriented epithelium, and LGSOC organoids forming denser and more complex structures with several lumens. To our knowledge such morphological comparison between ovarian cancer and fallopian tube organoids has not yet been described. Nevertheless, these results further solidify the notion that patient-derived organoids mimic the morphology of their tissue of origin [54], seeing that fallopian tubes are hollow organs [84] and low-grade serous carcinomas are known to possess solid components and sometimes display a complex structure [85].

Besides their different morphology, tumor and fallopian tube organoids also displayed distinct formation rates. Upon initial seeding FT organoids were observed sooner than LGSOC ones and following splitting at similar ratios the former reached confluency much faster than the latter. In fact, IF analysis using Ki-67, a widely used marker of cell proliferation [86], revealed that FT organoids had a higher proportion of proliferating cells when compared to LGSOC organoids. This implies that, in some cases, normal organoids might actually grow faster than their tumor counterparts. Although being counterintuitive, normal cells may have a growth advantage over cancer cells due to the genetically unstable nature of the latter, which results in an increased rate of mitotic failures and, consequently, increased apoptotic rates [47,87,88]. Indeed, contamination of normal epithelial tissue in cultures of tumor organoids has been reported as a challenge in the development of "pure" organoids derived from primary prostate cancer, as well as from colorectal and pancreas cancers, since tumor cells tend to be overgrown by normal cells [87,88].

Among the many applications of patient-derived tumor organoids, their possible use as a tool to predict tumor treatment responses takes us one step closer to implementing personalized medicine strategies in the clinic [83,89]. As such, one of the main goals of this project was to assess the sensitivity

profile of ovarian cancer organoids to drugs commonly used as therapy for EOC. High-grade serous ovarian carcinoma frequently displays mutations in *BRCA* genes [13] and it has been suggested that sensitivity to anti-cancer drugs might be related to expression of *BRCA1/2* mRNA [67,68]. Therefore, we intended to correlate drug sensitivity profiles to expression of *BRCA* and expected that these transcripts could represent a novel biomarker for predicting therapy response in HGSOC patients. However, as already stated, we only succeeded in generating organoids of low-grade serous ovarian carcinoma. These tumors typically do not harbor any defects in *BRCA* genes [3,27], so it was not possible to evaluate the potential of *BRCA* transcripts as predictive biomarkers. Nonetheless, the sensitivity profiles of our LGSOC organoids to cisplatin and olaparib did reflect what is usually observed in the clinical setting. Low-grade tumors tend to be insensitive to chemotherapy [26,27] and, in fact, our organoids appeared to be resistant to cisplatin, even at higher concentrations. It was not surprising that our tumor organoids were also not sensitive to olaparib since PARP inhibition is only effective in the presence of homologous recombination deficiency [33]. Therefore, patients with tumors like LGSOC that have a functional homologous recombination repair pathway will not benefit from the use of PARPi. Both high-grade and low-grade serous carcinomas are hypothesized to originate from the fallopian tube epithelium [17,30,31] so, as controls to the tumor organoids, we also assessed the sensitivity of healthy fallopian tube organoids to these drugs. As was expected, olaparib had no effect on the viability of FT organoids, for the same reason as described above for LGSOC organoids. On the other hand, upon exposure to high doses of cisplatin, the viability of these organoids was severely affected, which somewhat reflects the known cytotoxicity of this agent to normal cells [90–92]. FT organoids were also sensitive to high concentrations of carboplatin but the effect of this drug was not as drastic as that of cisplatin, which is in agreement with reports of carboplatin being less toxic than its analog [13,90]. Collectively, these results demonstrate the possibility of using patient-derived cancer organoids to assess sensitivity to anti-tumor drugs, as had previously been described [58,64,65].

As a whole, the work here described strengthens the knowledge that patient-derived organoids faithfully recapitulate their tissue of origin, be it healthy or diseased. Overall, our organoids revealed a histology and expression of markers similar to the parent tissue, and their structural organization resembled that of human fallopian tubes and solid low-grade tumors. It was also possible to perform drug sensitivity assays on all generated organoids, and although no comparison could yet be made to patient's response, the sensitivity profiles to chemotherapy and PARPi reflected what is usually expected for LGSOC, which supports the idea that organoids can be used as reliable preclinical platforms to predict treatment response. Nevertheless, improvements need to be made in the drug sensitivity assays to reduce variability between replicates. A major issue we faced was the heterogeneity of organoid density between wells upon plating, which affected the drug sensitivity results. Ways to overcome this problem may be to increase the number of replicates, to improve the homogenization of the organoid suspension after organoid dissociation or to use an alternative assay to measure cell viability before and after treatment, allowing for a normalization of the results [93].

Seeing the aim of this project was to assess the use of tumor-derived organoids as a model to predict therapy response in high-grade serous ovarian carcinoma, it remains necessary to develop organoids from this tumor type and future work will thus require the availability of HGSOC samples.

6. Main Conclusions and Future Perspectives

In this project, patient-derived organoids were successfully generated from a low-grade serous ovarian carcinoma and human fallopian tubes. All organoid lines were maintained for over 7 weeks, during which we performed morphological characterizations of the organoids and evaluated their sensitivity to anti-cancer drugs.

Standard H&E staining of LGSOC and FT organoids revealed similar histological features between them and the original tissue, tumor and healthy, respectively. Organoids also retained expression of most protein markers, being positive for PAX8 and WT1, and displaying a p53 wild-type staining pattern. Immunofluorescent staining highlighted clear structural differences between tumor and FT organoids, as well as distinct proliferation rates. LGSOC organoids showed no sensitivity to cisplatin nor the PARPi olaparib, as is expected for this type of cancer. As for FT organoids, they lacked therapeutic sensitivity to olaparib but elevated concentrations of cisplatin seemed to be lethal, whereas the effect of carboplatin on organoid viability was not as severe, which reflects its lesser toxicity to normal tissues.

In sum, the results here described further support the hypothesis that patient-derived tumor organoids replicate many characteristics of their original tumors and may be used as a preclinical tool to assess tumor response to therapy, eventually allowing for tailored therapeutic regimens to individual patients.

As high-grade serous ovarian carcinoma samples become available in the future, it is anticipated that organoids from that OC type will be successfully developed and maintained. We expect to show proof-of-principle that drug response and DNA repair activity in HGSOC-derived organoids correlate with the expression of *BRCA1/2* transcripts in the original tumors, thus showing that *BRCA* mRNA might be used as a novel predictive biomarker for high-grade serous ovarian carcinoma.

7. References

1. Bray F, Ferlay J, Soerjomataram I. Global Cancer Statistics 2018: GLOBOCAN Estimates of Incidence and Mortality Worldwide for 36 Cancers in 185 Countries. CA Cancer J Clin. 2018;68(6):394–424.
2. Prat J, D'Angelo E, Espinosa I. Ovarian carcinomas: at least five different diseases with distinct histological features and molecular genetics. Hum Pathol. 2018;80:11–27.
3. Lheureux S, Braunstein M, Oza AM. Epithelial Ovarian Cancer: Evolution of Management in the Era of Precision Medicine. CA Cancer J Clin. 2019;69:280–304.
4. Assis J, Pereira D, Nogueira A, Medeiros R. Ovarian Cancer Overview: Molecular Biology and Its Potential Clinical Application. In: Devaja O, Papadopoulos A, editors. Ovarian Cancer - From Pathogenesis to Treatment. IntechOpen; 2018. p. 57–82.
5. Stewart C, Ralyea C, Lockwood S. Ovarian Cancer: An Integrated Review. Semin Oncol Nurs. 2019;35(2):151–6.
6. Kurman RJ, Carcangiu ML, Herrington CS, Young RH. WHO Classification of Tumours of Female Reproductive Organs. 4th ed. IARC; 2014.
7. SPG. Cancro Ginecológico - Consensos Nacionais 2020. 2020.
8. Lheureux S, Gourley C, Vergote I, Oza AM. Epithelial ovarian cancer. Lancet. 2019;393(10177):1240–53.
9. Zhang J, Silva ES, Sood AK, Liu J. Ovarian Epithelial Carcinogenesis. In: Zheng W, Fadare O, Quick CM, Shen D, Guo D, editors. Gynecologic and Obstetric Pathology. Springer, Singapore; 2019. p. 121–39.
10. Ahmed N, Kadife E, Raza A, Short M, Jubinsky PT, Kannourakis G. Ovarian Cancer, Cancer Stem Cells and Current Treatment Strategies: A Potential Role of Magmas in the Current Treatment Methods. Cells. 2020;9(3):719.
11. Hirst J, Crow J, Godwin A. Ovarian Cancer Genetics: Subtypes and Risk Factors. In: Devaja O, Papadopoulos A, editors. Ovarian Cancer - From Pathogenesis to Treatment. IntechOpen; 2018. p. 3–38.
12. Aubrey BJ, Strasser A, Kelly GL. Tumor-suppressor functions of the TP53 pathway. Cold Spring Harb Perspect Med. 2016 May 1;6(5).
13. Lisio M-A, Fu L, Goyeneche A, Gao Z, Telleria C. High-Grade Serous Ovarian Cancer: Basic Sciences, Clinical and Therapeutic Standpoints. Int J Mol Sci. 2019;20(4):952.
14. Venkitaraman AR. Cancer susceptibility and the functions of BRCA1 and BRCA2. Cell. 2002;108(2):171–82.
15. Singh N, McCluggage WG, Gilks CB. High-grade serous carcinoma of tubo-ovarian origin: recent developments. Vol. 71, Histopathology. Blackwell Publishing Ltd; 2017. p. 339–56.
16. Liliac L, Luisa Carcangiu M, Canevari S, Căruntu ID, Apostol DGC, Danciu M, et al. The value of PAX8 and WT1 molecules in ovarian cancer diagnosis. Rom J Morphol Embryol. 2013;54(1):17–27.
17. Klotz DM, Wimberger P. Cells of origin of ovarian cancer: ovarian surface epithelium or fallopian tube ? Arch Gynecol Obstet. 2017;296(6):1055–62.
18. Zhang S, Dolgalev I, Ran H, Zhang T, Levine DA, Neel BG. Both fallopian tube and ovarian surface epithelium are cells-of-origin for high-grade serous ovarian carcinoma. Nat Commun. 2019;10:5367.
19. Karst AM, Levanon K, Drapkin R. Modeling high-grade serous ovarian carcinogenesis from the fallopian tube. Proc Natl Acad Sci U S A. 2011;108(18):7547–52.

20. Moss EL, Hollingworth J, Reynolds TM. The role of CA125 in clinical practice. J Clin Pathol. 2005 Mar 1;58(3):308–12.

21. Scholler N, Urban N. CA125 in Ovarian Cancer. Biomark Med. 2007 Dec 17;1(4):513–23.

22. Budiana ING, Angelina M, Pemayun TGA. Ovarian cancer: Pathogenesis and current recommendations for prophylactic surgery. J Turkish-German Gynecol Assoc. 2019;20(1):47–54.

23. Chang X, Ye X, Dong L, Cheng H, Cheng Y, Zhu L, et al. Human epididymis protein 4 (HE4) as a serum tumor biomarker in patients with ovarian carcinoma. Int J Gynecol Cancer. 2011 Jun 1;21(5):852–8.

24. James NE, Chichester C, Ribeiro JR. Beyond the biomarker: Understanding the diverse roles of human epididymis protein 4 in the pathogenesis of epithelial ovarian cancer. Vol. 8, Frontiers in Oncology. Frontiers Media S.A.; 2018. p. 124.

25. Della Pepa C, Tonini G, Santini D, Losito S, Pisano C, Di Napoli M, et al. Low Grade Serous Ovarian Carcinoma: From the molecular characterization to the best therapeutic strategy. Cancer Treat Rev. 2015;41(2):136–43.

26. Kaldawy A, Segev Y, Lavie O, Auslender R, Sopik V, Narod SA. Low-grade serous ovarian cancer: A review. Gynecol Oncol. 2016;143(2):433–8.

27. Ricciardi E, Ataseven B, Heitz F, Prader S, Bommert M, Schneider S, et al. Low-grade Serous Ovarian Carcinoma. Geburtshilfe Frauenheilkd. 2018;78(10):972–6.

28. Vang R, Shih IM, Kurman RJ. Ovarian low-grade and high-grade serous carcinoma: Pathogenesis, clinicopathologic and molecular biologic features, and diagnostic problems. Adv Anat Pathol. 2009;16(5):267–82.

29. Forgó E, Longacre TA. Low grade serous carcinoma. Pathology Outlines website. 2020. Available from: http://www.pathologyoutlines.com/topic/ovarytumorserouscarcinomalg.html

30. Wang Y, Hong S, Mu J, Wang Y, Lea J, Kong B, et al. Tubal Origin of "Ovarian" Low-Grade Serous Carcinoma: A Gene Expression Profile Study. J Oncol. 2019;2019.

31. Li J, Abushahin N, Pang S, Xiang L, Chambers SK. Tubal origin of "ovarian" low-grade serous carcinoma. Mod Pathol. 2011;24:1488–99.

32. Gadducci A, Cosio S. Therapeutic approach to low-grade serous ovarian carcinoma: State of art and perspectives of clinical research. Cancers (Basel). 2020;12(5).

33. Curtin NJ. DNA repair dysregulation from cancer driver to therapeutic target. Nat Rev Cancer. 2012;12(12):801–17.

34. Gee ME, Faraahi Z, McCormick A, Edmondson RJ. DNA damage repair in ovarian cancer: Unlocking the heterogeneity. J Ovarian Res. 2018;11(1):1–12.

35. Damia G, Broggini M. Platinum resistance in ovarian cancer: Role of DNA repair. Cancers (Basel). 2019;11(1):1–15.

36. Rocha CRR, Silva MM, Quinet A, Cabral-Neto JB, Menck CFM. DNA repair pathways and cisplatin resistance: An intimate relationship. Clinics. 2018;73(8):1–10.

37. Lord CJ, Ashworth A. The DNA damage response and cancer therapy. Nature. 2012;481(7381):287–94.

38. da Cunha Colombo Bonadio RR, Fogace RN, Miranda VC, Diz MDPE. Homologous recombination deficiency in ovarian cancer: A review of its epidemiology and management. Clinics. 2018;73:1–6.

39. Vítor AC, Huertas P, Legube G, de Almeida SF. Studying DNA Double-Strand Break Repair: An Ever-Growing Toolbox. Front Mol Biosci. 2020;7(February):1–16.

40. Kubelac P, Auguste A, Genestie C, Mesnage S, Le Formal A, Achimas-Cadariu P, et al. Changes in DNA damage response markers with treatment in advanced ovarian cancer. Cancers (Basel). 2020;12(3):707.

41. De Picciotto N, Cacheux W, Roth A, Chappuis PO, Labidi-Galy SI. Ovarian cancer: Status of homologous recombination pathway as a predictor of drug response. Crit Rev Oncol Hematol. 2016;101:50–9.

42. Stefanou DT, Bamias A, Episkopou H, Kyrtopoulos SA, Likka M, Kalampokas T, et al. Aberrant DNA Damage Response Pathways May Predict the Outcome of Platinum Chemotherapy in Ovarian Cancer. PLoS One. 2015;10(2):1–19.

43. Ceccaldi R, Sarangi P, D'Andrea AD. The Fanconi anaemia pathway: New players and new functions. Nat Rev Mol Cell Biol. 2016;17(6):337–49.

44. D'Andrea AD. BRCA1: A Missing Link in the Fanconi Anemia/BRCA Pathway. Cancer Discov. 2013;3(4):376–8.

45. Lord CJ, Tutt ANJ, Ashworth A. Synthetic lethality and cancer therapy: Lessons learned from the development of PARP inhibitors. Annu Rev Med. 2015;66(October 2014):455–70.

46. Franzese E, Centonze S, Diana A, Carlino F, Guerrera LP, Di Napoli M, et al. PARP inhibitors in ovarian cancer. Cancer Treat Rev. 2019;73(October 2018):1–9.

47. Drost J, Clevers H. Organoids in cancer research. Nat Rev Cancer. 2018;18(7):407–18.

48. Yang H, Sun L, Liu M, Mao Y. Patient-derived organoids: A promising model for personalized cancer treatment. Gastroenterol Rep. 2018;6(4):243–5.

49. WHO. WHO report on cancer: setting priorities, investing wisely and providing care for all. World Health. 2020.

50. Fan H, Demirci U, Chen P. Emerging organoid models: Leaping forward in cancer research. J Hematol Oncol. 2019;12(1):1–10.

51. Maru Y, Hippo Y. Current Status of Patient-Derived Ovarian Cancer Models. Cells. 2019;8(5):505.

52. Maru Y, Tanaka N, Itami M, Hippo Y. Efficient use of patient-derived organoids as a preclinical model for gynecologic tumors. Gynecol Oncol. 2019;154(1):189–98.

53. Kim S, Choung S, Sun RX, Ung N, Hashemi N, Fong EJ, et al. Comparison of Cell and Organoid-Level Analysis of Patient-Derived 3D Organoids to Evaluate Tumor Cell Growth Dynamics and Drug Response. SLAS Discov. 2020;25(7):744–54.

54. Dumont S, Jan Z, Heremans R, Van Gorp T, Vergote I, Timmerman D. Organoids of epithelial ovarian cancer as an emerging preclinical in vitro tool: A review. J Ovarian Res. 2019;12(1):1–11.

55. Clevers H. Modeling Development and Disease with Organoids. Cell. 2016;165(7):1586–97.

56. Kopper O, Witte CJ De, Lõhmussaar K, Valle-Inclan JE, Hami N, Kester L, et al. An organoid platform for ovarian cancer captures intra- and interpatient heterogeneity. Nat Med. 2019;25(5):838–49.

57. Pasch CA, Favreau PF, Yueh AE, Babiarz CP, Gillette AA, Sharick JT, et al. Patient-derived cancer organoid cultures to predict sensitivity to chemotherapy and radiation. Clin Cancer Res. 2019;25(17):5376–87.

58. Driehuis E, Kretzschmar K, Clevers H. Establishment of patient-derived cancer organoids for drug-screening applications. Nat Protoc. 2020;15(10):3380–409.

59. Aboulkheyr Es H, Montazeri L, Aref AR, Vosough M, Baharvand H. Personalized Cancer Medicine: An Organoid Approach. Trends Biotechnol. 2018;36(4):358–71.

60. Chen H, Gotimer K, De Souza C, Tepper CG, Karnezis AN, Leiserowitz GS, et al. Short-term organoid culture for drug sensitivity testing of high-grade serous carcinoma. Gynecol Oncol. 2020;157(3):783–92.

61. de Witte CJ, Espejo Valle-Inclan J, Hami N, Lõhmussaar K, Kopper O, Vreuls CPH, et al. Patient-Derived Ovarian Cancer Organoids Mimic Clinical Response and Exhibit Heterogeneous Inter- and Intrapatient Drug Responses. Cell Rep. 2020;31(11).

62. Nanki Y, Chiyoda T, Hirasawa A, Ookubo A, Itoh M, Ueno M, et al. Patient-derived ovarian cancer organoids capture the genomic profiles of primary tumours applicable for drug sensitivity and resistance testing. Sci Rep. 2020;10(1):1–11.

63. Hoffmann K, Berger H, Kulbe H, Thillainadarasan S, Mollenkopf H, Zemojtel T, et al. Stable expansion of high-grade serous ovarian cancer organoids requires a low-Wnt environment. EMBO J. 2020;39(6):1–23.

64. Hill SJ, Decker B, Roberts EA, Horowitz NS, Muto MG, Jr MJW, et al. Prediction of DNA Repair Inhibitor Response in Short-Term Patient-Derived Ovarian Cancer Organoids. Cancer Discov. 2018;8(11):1404–21.

65. Maenhoudt N, Defraye C, Boretto M, Jan Z, Heremans R, Boeckx B, et al. Developing Organoids from Ovarian Cancer as Experimental and Preclinical Models. Stem Cell Reports. 2020;14(4):717–29.

66. Vaz F, Pereira D. 100 Perguntas chave no Cancro do Ovário. Lisboa: Permanyer Portugal; 2015.

67. Tsibulak I, Wieser V, Degasper C, Shivalingaiah G, Wenzel S, Sprung S, et al. BRCA1 and BRCA2 mRNA-expression prove to be of clinical impact in ovarian cancer. Br J Cancer. 2018;119(6):683–92.

68. Mądry R, Christensen RD, Berek JS, Dørum A, Tinker A V, Bois A, et al. Niraparib Maintenance Therapy in Platinum-Sensitive, Recurrent Ovarian Cancer. N Engl J Med. 2016;375(22):2157–64.

69. Kaushik G, Ponnusamy MP, Batra SK. Current Status of Three-Dimensional Organoids as Preclinical Models. Stem Cells. 2018 Sep 1;36(9):1329–40.

70. Fang Y, Eglen RM. Three-Dimensional Cell Cultures in Drug Discovery and Development. SLAS Discov. 2017 Jun 1;22(5):456–72.

71. Promega. Technical Bulletin - CellTiter-Glo® Luminescent Cell Viability Assay. Available from: https://worldwide.promega.com/products/cell-health-assays/cell-viability-and-cytotoxicity-assays/celltiter_glo-luminescent-cell-viability-assay/?catNum=G7570

72. Yang L, Yang S, Li X, Li B, Li Y, Zhang X, et al. Tumor organoids: From inception to future in cancer research. Cancer Lett. 2019;454:120–33.

73. AggreWell™ Microwell Plates - Spheroids and Embryoid Bodies. Available from: https://www.stemcell.com/products/brands/aggrewell.html

74. 3D Cell Culture Assays | Single Cells, Spheroids, Organoids | ibidi. Available from: https://ibidi.com/content/397-3d-cell-culture-assays#spheroid_organoid_culture

75. Zanoni M, Cortesi M, Zamagni A, Arienti C, Pignatta S, Tesei A. Modeling neoplastic disease with spheroids and organoids. Vol. 13, Journal of Hematology and Oncology. BioMed Central; 2020. p. 97.

76. Kaushik G, Ponnusamy MP, Batra SK. Concise Review: Current Status of Three-Dimensional Organoids as Preclinical Models. Stem Cells. 2018 Sep 1;36(9):1329–40.

77. Corning. Corning® Matrigel® Matrix. Available from: https://www.corning.com/worldwide/en/products/life-sciences/products/surfaces/matrigel-matrix.html

78. Rogers H, Letchford L, Vieira S, Garcia-Casado M, Fekry-Troll M, Beaver C, et al. Passaging cancer organoid cultures. 2020 Jul 7; Available from: https://dx.doi.org/10.17504/protocols.io.bfe3jjgn

79. Ruchinskas A, Clinton J. Protocol for the thawing, expansion, and cryopreservation of mouse small intestinal organoids. 2019. Available from: https://www.atcc.org/~/media/Attachments/Application%20Notes/Protocol%20for%20the%20thawing%20organoids.ashx

80. Urbischek M, Rannikmae H, Foets T, Ravn K, Hyvönen M, de la Roche M. Organoid culture media formulated with growth factors of defined cellular activity. Sci Rep. 2019 Dec 1;9(1):1–11.

81. AMS Biotechnology. Organoid Culture Handbook. Available from: www.amsbio.com

82. Kessler M, Hoffmann K, Brinkmann V, Thieck O, Jackisch S, Toelle B, et al. The Notch and Wnt pathways regulate stemness and differentiation in human fallopian tube organoids. Nat Commun. 2015;6(May):1–11.

83. Porter RJ, Murray GI, Mclean MH. Current concepts in tumour-derived organoids. Br J Cancer. 2020;123(July):1209–18.

84. Han J, Sadiq NM. Anatomy, Abdomen and Pelvis, Fallopian Tube. StatPearls. StatPearls Publishing; 2019. Available from: http://www.ncbi.nlm.nih.gov/pubmed/31613440

85. Gadducci A, Cosio S. Therapeutic approach to low-grade serous ovarian carcinoma: State of art and perspectives of clinical research. Cancers (Basel). 2020 May 1;12(5):1336.

86. Juríková M, Danihel Ľ, Polák Š, Varga I. Ki67, PCNA, and MCM proteins: Markers of proliferation in the diagnosis of breast cancer. Acta Histochem. 2016 Jun 1;118(5):544–52.

87. Weeber F, Ooft SN, Dijkstra KK, Voest EE. Tumor Organoids as a Pre-clinical Cancer Model for Drug Discovery. Cell Chem Biol. 2017;24(9):1092–100.

88. Karthaus WR, Iaquinta PJ, Drost J, Gracanin A, Van Boxtel R, Wongvipat J, et al. Identification of multipotent luminal progenitor cells in human prostate organoid cultures. Cell. 2014 Sep 25;159(1):163–75.

89. Nagle PW, Plukker JTM, Muijs CT, van Luijk P, Coppes RP. Patient-derived tumor organoids for prediction of cancer treatment response. Semin Cancer Biol. 2018 Dec 1;53:258–64.

90. Mikuła-Pietrasik J, Witucka A, Pakuła M, Uruski P, Begier-Krasińska B, Niklas A, et al. Comprehensive review on how platinum- and taxane-based chemotherapy of ovarian cancer affects biology of normal cells. Cell Mol Life Sci. 2019 Feb 28;76(4):681–97.

91. Li Y, Zhang X, Yang X, Liu J, Li L, Ma W, et al. Differential effects of ginkgol C17:1 on cisplatin-induced cytotoxicity: Protecting human normal L02 hepatocytes versus sensitizing human hepatoma HepG2 cells. Oncol Lett. 2019 Mar 1;17(3):3181–90.

92. Florea AM, Büsselberg D. Cisplatin as an anti-tumor drug: Cellular mechanisms of activity, drug resistance and induced side effects. Cancers (Basel). 2011 Mar;3(1):1351–71.

93. Whyard T, Liu J, Darras FS, Waltzer WC, Romanov V. Organoid model of urothelial cancer: cancer research. Biotechniques. 2020;69(3):193–9.

8. Appendix – H&E staining of LGSOC and FT organoids

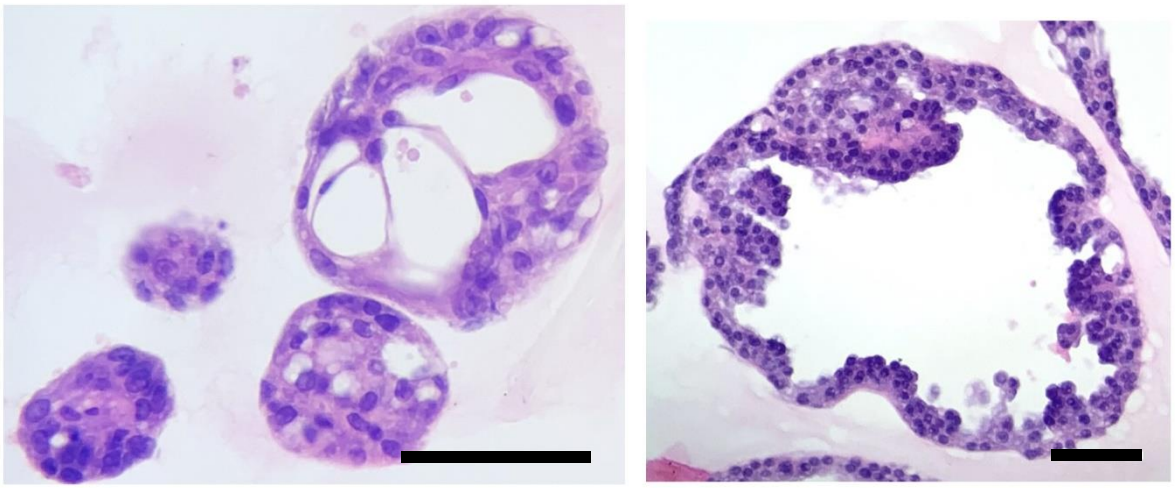

Figure 8.1 | Low-grade serous ovarian carcinoma (LGSOC) organoids morphologically mimic the tumor tissue from which they were derived. Standard H&E staining of the LGSOC organoids revealed globally spherical structures with cribriform architecture (left), a feature of complexity, and micropapillary projections (right), a typical feature of LGSOCs. At different timepoints during culture, organoids were found in distinct stages of maturation, with differences in size and differentiation (passage 2, left vs passage 7, right). Scale bar, 100 µm.

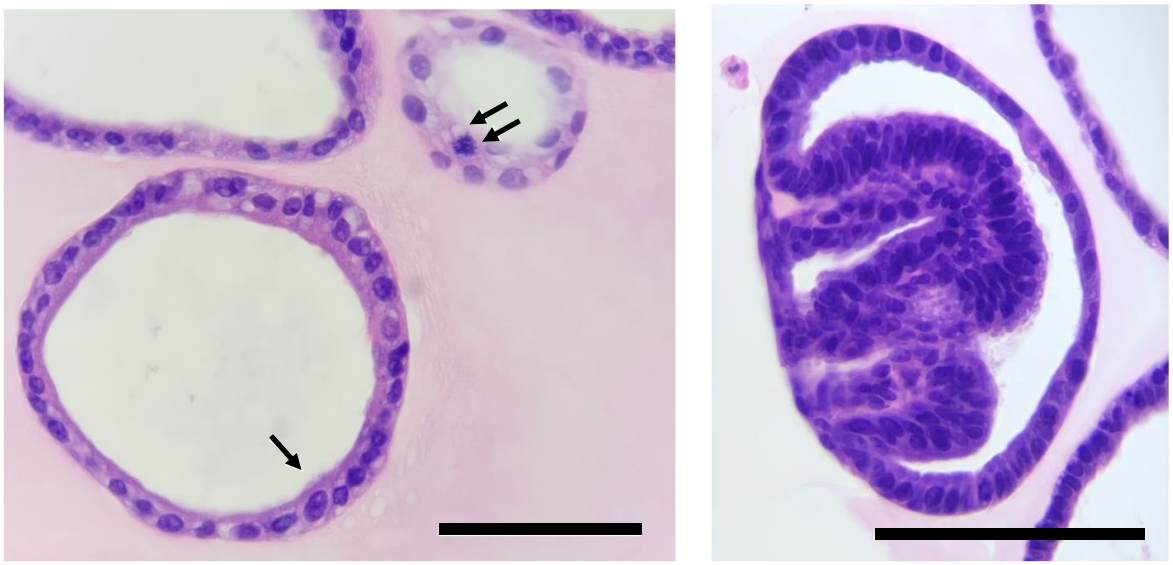

Figure 8.2 | Fallopian tube (FT) organoids morphologically mimic the normal tissue from which they were derived. Standard H&E staining of the FT organoids revealed the presence of both secretory and ciliated cells (arrow), as well as the presence of occasional mitotic figures (double arrow). Several organoids also developed epithelium folds (right), an important feature of normal human fallopian tube epithelia. Scale bar, 100 µm.